Brain-targeted liposomes loaded with monoclonal antibodies reduce alpha-synuclein aggregation and improve behavioral symptoms of Parkinson's disease

*Mor Sela[1, #], Maria Poley[1, #], Patricia Mora-Raimundo[1, #], Shaked Kagan[1], Aviram Avital[2], Maya Kaduri[1], Gal Chen[1,3], Omer Adir[2], Adi Rozencweig[1], Yfat Weiss[4], Ofir Sade[4], Yael Leichtmann-Bardoogo[5], Lilach Simchi[6], Shlomit Age-Mizrachi[6], Batia Bell[8], Yoel Yeretz-Peretz[8], Aviv Zaid Or[5,7], Ashwani Choudhary[9], Idan Rosh[9], Diogo Cordeiro[9], Stav Choen-Adiv[10], Yevgeny Berdichevsky[10], Anas Ode[14], Jeny Shklover[1], Janna Shainsky-Roitman[1], Joshua E. Schroeder[11], Dov Hershkovitz[12,13], Peleg Hasson[14], Avraham Ashkenazi[5,10], Shani Stern[9], Tal Laviv[5,7], Ayal Ben-Zvi[8], Avi Avital[6], Uri Ashery[4,5], Ben M. Maoz[5,15-17] and Avi Schroeder[1, *]*

[1]The Louis Family Laboratory for Targeted Drug Delivery and Personalized Medicine Technologies, Department of Chemical Engineering, Technion – Israel Institute of Technology, Haifa 32000, Israel
[2]The Norman Seiden Multidisciplinary Program for Nanoscience and Nanotechnology, Technion – Israel Institute of Technology, Haifa 32000, Israel
[3]The Interdisciplinary Program for Biotechnology, Technion - Israel Institute of Technology, Haifa 32000, Israel
[4]School of Neurobiology, Biochemistry and Biophysics, George S. Wise Faculty of Life Sciences, Sagol School of Neuroscience, Tel Aviv University, Tel Aviv 6997801, Israel
[5]Sagol School of Neuroscience, Tel Aviv University, Tel Aviv 6997801, Israel
[6]Department of Occupational Therapy, Faculty of Social Welfare and Health Sciences, University of Haifa, Haifa 3498838, Israel
[7]Department of Physiology and Pharmacology, Faculty of Medicine, Tel Aviv University, Tel Aviv 6997801, Israel
[8]Department of Developmental Biology and Cancer Research, The Institute for Medical Research Israel-Canada, Faculty of Medicine, The Hebrew University of Jerusalem, Jerusalem 9190500, Israel
[9]Sagol Department of Neurobiology, Faculty of Natural Sciences, University of Haifa, Haifa 3498838, Israel
[10]The Department of Cell and Developmental Biology, Faculty of Medicine, Tel Aviv University, Tel Aviv 6997801, Israel

This article has been accepted for publication and undergone full peer review but has not been through the copyediting, typesetting, pagination and proofreading process, which may lead to differences between this version and the Version of Record. Please cite this article as doi: 10.1002/adma.202304654.

[11]Spine Unit, Orthopedic Complex, Hadassah Hebrew University Medical Center, Kiryat Hadassah, POB 12000, Jerusalem 9190500, Israel
[12]Department of Pathology, Tel Aviv Sourasky Medical Center, Tel Aviv 6997801, Israel
[13]Sackler Faculty of Medicine, Tel Aviv University, Tel Aviv 6997801, Israel
[14]Department of Genetics and Developmental Biology, The Rappaport Faculty of Medicine and Research Institute, Technion – Israel Institute of Technology, Haifa 32000, Israel
[15]Department of Biomedical Engineering, Tel Aviv University, Tel Aviv 6997801, Israel
[16]The Center for Nanoscience and Nanotechnology, Tel Aviv University, Tel Aviv 6997801, Israel [17]Sagol Center for Regenerative Medicine, Tel Aviv University, Tel Aviv 6997801, Israel

*** Corresponding author**
avids@technion.ac.il# **These authors contributed equally**
Keywords: brain targeting, lipid nanoparticles, neuroinflammation, Parkinson's disease, central nervous system.

Abstract –

Monoclonal antibodies (mAbs) hold promise for treating Parkinson's disease (PD), but their therapeutic use is hindered by poor delivery to the brain. In this study, we demonstrate that brain-targeted liposomes (BTL) enhance the delivery of mAbs across the blood-brain-barrier (BBB) and into neurons, thereby improving the intracellular and extracellular treatment of the PD brain. BTL were decorated with transferrin to improve brain targeting through overexpressed transferrin-receptors on the BBB during PD. The BTL were loaded with SynO4, a mAb that inhibits alpha-synuclein (AS) aggregation, a pathological hallmark of PD. We show that 100-nm BTL cross human BBB models intact and were taken up by primary neurons. Inside the neurons, SynO4 is released from the nanoparticles and binds to its target, thereby reducing AS aggregation and increasing neuronal viability. *In-vivo*, intravenous administration of BTL led to a 7-fold increase of mAbs in brain cells, reducing AS aggregation and neuroinflammation. In addition, BTL treatments improved behavioral motor function and learning ability in mice, with a favorable safety profile. Targeted nanotechnologies are promising platforms for delivering medicines to treat brain neurodegeneration.

Introduction

Parkinson's disease (PD) affects nearly one percent of the population aged 60 and older, with limited treatment modalities. This neurodegenerative condition is primarily characterized by the degeneration of dopaminergic neurons in the midbrain substantia nigra (SN),[1] the result of which is debilitating motor symptoms such as tremors, poor gate, and speech functions, which deteriorate as the disease progresses.[1b, 2] During PD, not only neurons but also microglia and astrocytes are impaired, leading to a loss of normal homeostatic and/or

acquisition of neurotoxic functions.[3] There is no single known cause of PD, however, genetic and environmental factors have been suggested to play a role in the disease's etiology.[4]

A pathological hallmark of PD is the presence of inclusion bodies (i.e., Lewy bodies), composed primarily of aggregated alpha-synuclein (AS).[5] AS mutations, such as A53T and A30P, lead to its abnormal accumulation and, consequently, oligomerization and aggregation.[6] AS is found in the brain in various conformations, from unfolded monomers to soluble oligomers and insoluble fibrils.[6] It has been suggested that the AS oligomers can either aggregate to form toxic β-sheet fibrils, leading to the propagation of AS pathology, or form structures that do not propagate but are, nevertheless, toxic.[7] Reducing AS oligomerization and aggregation has been suggested as a treatment for Parkinson's disease.[8] In line, monoclonal antibodies (mAbs), such as SynO4, were designed to bind epitopes in the non-amyloid β component and C-terminal regions of AS, thereby preventing their further aggregation.[9] However, SynO4 has poor brain penetration properties, and without a carrier, its activity is mainly extracellular.[10] These limitations can be overcome using nanoscale drug delivery systems, as they combine brain-targeting capabilities, with the ability to deliver multiple mAbs in each nanoparticle intracellularly.[11]

A primary hurdle for drugs targeting the brain is the blood-brain barrier (BBB). This physical and metabolic obstacle is composed of a monolayer of endothelial cells on the vascular lumen-side, while the pericytes and astrocytes on the basal-side provide support and directly interact with the endothelial cells. Tight junctions between endothelial cells restrict the passage of molecules into the brain, with access primarily regulated through receptor-mediated transcytosis.[12]

While nanoparticles are used as drug delivery systems for treating cancer[13] and targeting drugs to specific organs, such as the lungs and liver[14], their ability to penetrate the brain during PD needs to be studied. This can be achieved by adding targeting moieties to the outer surface of the nanoparticles, to enhance their BBB penetration.[11a, 15]

A promising approach to increase BBB penetration[16] in PD stems from the finding that in PD patients, the transferrin receptor (TfR1) is overexpressed on the BBB endothelial, allowing transcytosis across the barrier.[17]

We, therefore, hypothesized that conjugating transferrin (TF), a 76-KDa protein with affinity to the TfR1 receptor, to the liposome surface will enhance brain uptake of liposomes (**Figure 1A**).

Hence, in this study, we evaluated the ability of transferrin-conjugated liposomes loaded with SynO4 mAbs (herein brain-targeted liposomes, or BTL) to cross the BBB and deliver their therapeutic cargo to cells of the brain parenchyma, including endothelial, neurons, and glial cells. We further assessed the efficacy of these brain-targeted liposomes to reduce

neuroinflammation and slow PD progression in mice. Our findings support the use of targeted nanoparticles as systems for the targeted delivery of biologics to treat PD.

Results and Discussion

Synthesizing brain-targeted liposomes (BTL)

To cross the BBB, we engineered brain-targeted liposomes (BTL) by conjugating transferrin to the outer surface of 100-nm liposomes. BTL loaded with anti-AS mAbs were prepared through two main synthetic steps. First, SynO4 monoclonal antibodies were loaded into liposomes through a thin-film hydration process.[18] Then, transferrin was conjugated to amine-functionalized polyethylene glycol (PEG) extending from the outer surface of the liposomes, using EDC/NHS coupling chemistry[19] (**Figure 1B**).

The working temperature of the fabrication steps was selected to preserve the bioactivity of SynO4 throughout the process (T=45ºC; see methods, **Figure S1, and Figure S2**). 1,2-dipalmitoyl-sn-glycerol-3-phosphocholine (DPPC, 16:0, Tm=41°C) was chosen as the main lipid of the liposome composition at a molar of 60%, in addition to cholesterol (30mol%), 1,2-distearoyl-sn-glycero-3-phosphoethanolamine-N-[methoxy(polyethyleneglycol)-1000] (DSPE-PEG1000, 2.5mol%), and 1,2-distearoyl-sn-glycero-3-phosphoethanolamine-N-[amino(polyethyleneglycol)-2000] (DSPE-PEG2000-NH2, 2.5mol%). The average size of the BTL was 113.5±1.5 nm, with 33±6 antibodies loaded into each liposome and 95±23 TF-targeting molecules conjugated to their outer surface. (**Figures 1C, D, and S3**). The protein mass of the loaded SynO4 mAbs was 0.142 mg mAb/94.5 mg liposome-lipid and is comparable to the drug mass loaded into FDA-approved doxorubicin liposomes. This BTL composition allows the release of mAbs over the course of 48 hours at physiological conditions (p=0.0044) (**Figure S4**).

The untargeted, control, liposomes loaded with SynO4 mAbs had an average size of 114.3±0.3 nm, and a concentration of 73±10 SynO4 units per liposome (**Figures S3 and S5,** respectively). Notably, conjugating TF to the surface of the liposome displaced the SynO4 absorbed on the liposome's surface. BTL remained stable, and the mAb was biologically active, for 2 weeks, when held at 4°C, and for one week at 25°C (**Figure S6**).

Conjugating targeting moieties to the surface of nanoparticles was performed in a manner that does not affect the docking region within the targeting moiety and was not altered during the conjugation process. Therefore, we chose to conjugate the amine PEG linker to the carboxyl groups on the exterior of the TF moiety (**Movie S1**). Protein dynamics analysis demonstrated that each TF molecule has ~38 COOH binding sites to which the PEG entity can conjugate to, without compromising the biological binding site. The transferrin receptor binding site (TfR1-TF) consists of six main amino acids (His249, Tyr95, Asp63, Asp221, Asp356, Tyr188) that form multiple chemical interactions with TF. While Asp221 and Asp356 are the only amino acid residues that could potentially be conjugated with amine PEG, the likelihood of this occurrence is statistically low.[20]

To visualize the presence of TFs on the liposome surface, gold nanoparticles were conjugated to TFs, and imaged using cryogenic transmission electron microscopy (cryo-TEM). The gold nanoparticles (5 nm in diameter, dark objects in **Figure 1E**) can be seen in close proximity (<15 nm) to the outer surface of the liposomes (**Figure S7**), in agreement with their positioning on the distal end of the PEG2000 that extends from the liposome surface.

PEG molecules extending from the outer surface of nanoparticles can cause steric interference that prevents the targeting moieties from binding their biological target.[21] Only 3.8%±0.9% of the PEG chains extending from the BTL are conjugated to TF, while other PEG molecules extending from the liposome surface are capped with a non-binding methyl group on their distal side. These non-binding PEG molecules improve the liposomes' steric stability and extend circulation time. [22]

To address the steric hindrance caused by PEG, we studied the uptake of liposomes with TF conjugated to short (1000) and/or long (2000) PEG moieties, by human brain endothelial cells (hCMEC/D3) (**Figure 1F**). We found that endothelial uptake is greater when nanoparticles have TF molecules that are conjugated to a PEG moiety that is longer than the neighboring unconjugated PEG. Specifically, particles to which TF was conjugated to PEG2000 (PEG2000-TF) combined with unconjugated PEG1000 had superior endothelial uptake than particles with unconjugated PEG2000 (p<0.0001). Given these findings, we hypothesize that when the length of an unconjugated PEG-lipid is a similar to that of a targeting-ligand-displaying PEG lipid, the neighboring PEG molecules exert a steric hindrance effect, inhibiting the targeting ligand from efficiently interacting with its receptor. When the unconjugated PEG-lipid is shorter than the PEG used to conjugate the targeting moiety, this steric hindrance is reduced, and cellular uptake is improved. Accordingly, we continued with a PEG2000-TF/PEG1000 formulation for the rest of the study. Interestingly, we and others have observed that PEG extending from the surface of liposomes has a favorable effect on uptake by neurons.[23]

To optimize the number of TF moieties per nanoparticle, we screened liposomes with an increasing number of TFs on their surface (**Figure S8**). The uptake of transferrin-conjugated liposomes without SynO4 mAbs (herein BTL (empty)) by endothelial cells improved as the number of TFs conjugated to the surface of the liposome increased (p<0.0001). Maximal endothelial uptake was achieved at a TF concentration of 109±11 per liposome (achieved by adding 20 mg/ml TF during the formulation process), at which the surface of the liposome was saturated. Having this said, the optimal BTL in terms of financial cost vs. benefit of cell

uptake were liposomes with 95±23 TF units (achieved by adding only 10 mg/ml TF during the formulation process, see Methods and **Figure S9**).

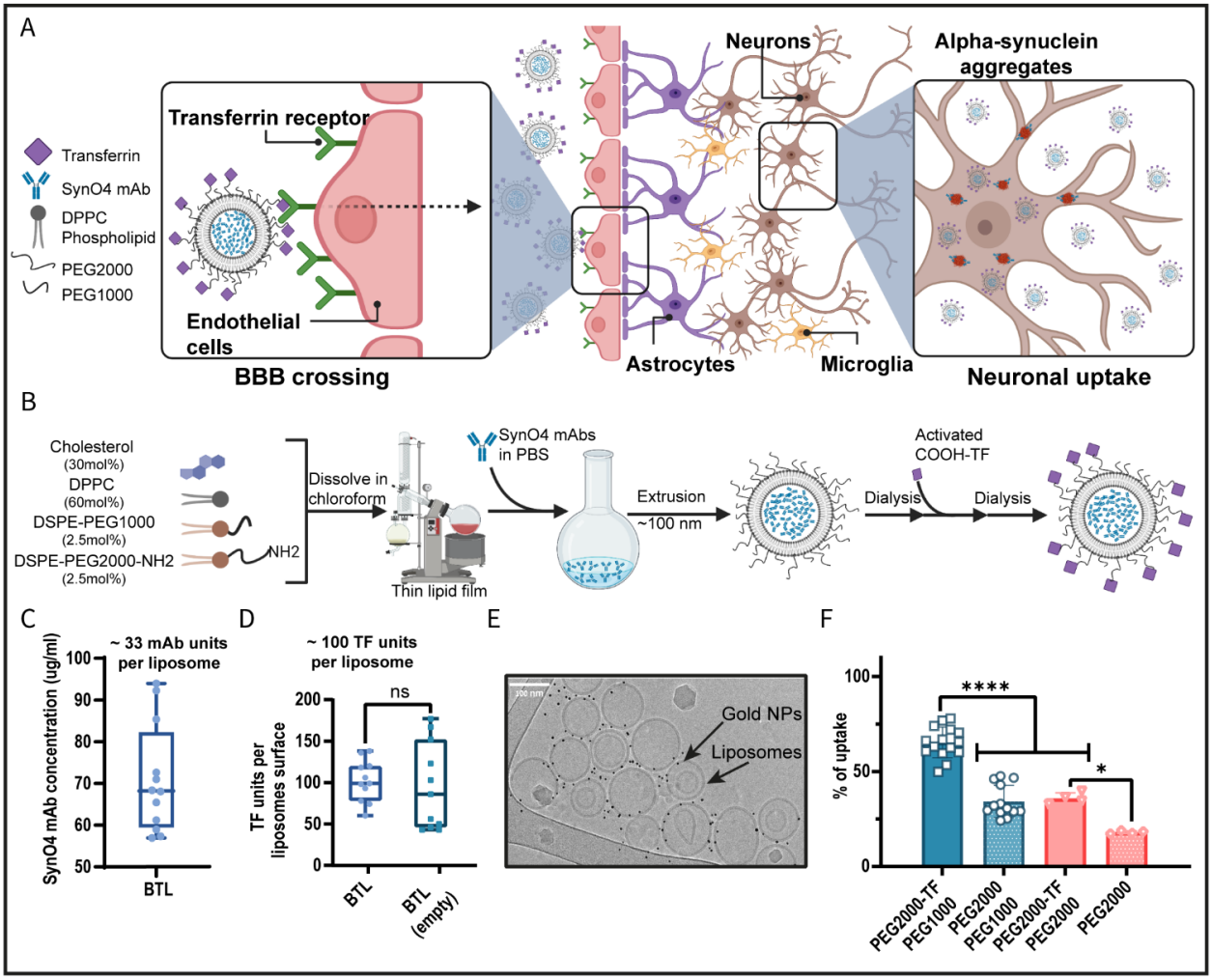

Figure 1. Synthesizing brain-targeted liposomes loaded with SynO4 mAb. (A). Schematic illustration of the therapeutic mode of action. Through receptor-mediated transcytosis, liposomes carrying SynO4 mAbs cross the BBB and are taken up by damaged neuron cells; the mAbs are then released and go on to target AS aggregates, thereby preventing neuron cell death. **(B).** Schematic diagram of the synthesis of BTL. **(C).** Quantification of the encapsulated SynO4 mAbs' concentration in BTL by ELISA assay. **(D).** Evaluation of the amount of transferrin units per liposomes' surface by BCA protein assay. **(E).** Cryogenic transmission electron microscopy (cryo-TEM) of gold nanoparticles (GNPs) linked to BTL (empty) (scale bar: 100 nm). **(F).** *In-vitro* cellular uptake of targeted PEGlated liposomes in hCMEC/D3 cells; the uptake efficiency of each liposomal formulation was assessed by FACS analysis. The results of C and D (at least 12 independent repetitions) and F (at least 4 independent repetitions performed in three replicates) are presented as mean±SD. Two-tailed unpaired Student's t-test was used for the statistical analysis of D, and One-way ANOVA was used for the statistical analysis of F, with multiple comparisons test adjusted *p*-value; **p*=0.0111, *****p*<0.0001.

BTL cross the blood-brain-barrier (BBB)

We assessed the ability of BTL to cross an *in-vitro* BBB model of the neurovascular unit (NVU) and their integrity after crossing the BBB. This model system is composed of a Transwell\Chip plate containing a compartment of induced pluripotent stem cells (iPSC) derived human microvascular endothelial cells (BMECs) placed, in a noncontact manner,

atop a basolateral compartment of primary cortical neurons and astrocytes (**Figure 2A**). The degree of BTL transport across the endothelial monolayers was determined by measuring the liposomal content in the media on the basolateral side of the BBB. We found that the permeability of the BTL across the monolayer increased over time from the donor to the acceptor cell (**Figure 2B**), without affecting the integrity of the tight junctions in the endothelial monolayer (**Figure S10**). Cryo-TEM analysis of the media on the basolateral side of the barrier confirmed that the BTL remained intact after crossing the BBB (**Figure 2C**). Furthermore, we conducted live imaging to monitor the passage of BTL across the BBB layers. Our observations show that particles were internalized by BMECs and migrated to the basolateral side of the BBB (**Figure S11 and Movie S2**).

To investigate the subcellular localization of BTL in capillary endothelial cells while crossing the BBB, we used dSTORM microscopy (**Figure 2D**).[24] Healthy mice were injected intravenously with AZDye 647-labeled BTL. Brains were fixed, and cortical tissue sections were immunolabeled with GLUT1 to identify the endothelium in capillary cross-sections and with LAMP1 to detect lysosome organelles within cells. Tissue dSTORM imaging confirmed BBB crossing of BTL. To further validate this finding, we tested a shorter exposure time point of 30 minutes to capture the BTL inside the endothelial cells (**Figure 2D(i)**). Additionally, BTL signals were observed in the brain parenchyma 6 hours post-injection (**Figure 2D(ii)**). Nano-scale localization of single molecules showed minimal colocalization of BTL with the lysosomal marker LAMP1. The fluorescent signal from the lysosome molecules (LAMP1) co-localized with only 1.7%±1.3% of the BTL fluorescent signal, suggesting that BTL are escaping lysosomal degradation once they have entered the endothelium.

Next, we determined the spatial and temporal dynamics associated with BTL entry into brain neurons (**Figures S12, 2E, and F**). We used in-utero electroporation of pCAG-EGFP plasmid at E14, to fluorescently label the excitatory layer 2/3 cortical cells within the mouse cerebral cortex.[25] GFP-positive mice were identified at birth and were left to mature until p30 when they underwent cranial window surgery.[26] To track BTL entry into cortical neurons *in vivo*, we used two-photon fluorescence lifetime imaging[26]. Then, we compared the fluorescence lifetime of neurites and cell bodies post-BTL injection. Two hours following injection, we observed small punctate structures characterized by shorter lifetimes along dendritic branches, whereas such structures were absent within cell bodies (**Figure 2E and F**; soma: 0.057Δns±0.03Δns (p=0.7293) vs. 0hr, and neurite: 0.306Δns±0.06Δns (p<0.0035) vs. 0hr). However, 5 hours post-injection, we were able to detect distinct punctate formations on both cell bodies and neurites, displaying lower lifetime values (**Figure 2E and F**; soma: 0.175Δns±0.03Δns (p<0.0012) vs. 0hr, and neurite: 0.487Δns±0.05Δns (p<0.0001) vs. 0hr). Our findings show that in a healthy cortex, BTL particles were internalized by neuronal processes within 2 hours and observed by cell bodies within 5 hours post-injection.

Overall, these findings suggest that BTL cross the BBB and evade lysosomal degradation in endothelial cells, then be taken up by neurons and cells in the brain parenchyma. BTL were found to distribute to other organs as well, mainly the liver and the kidneys, similarly to other reported nanoparticles.[27]

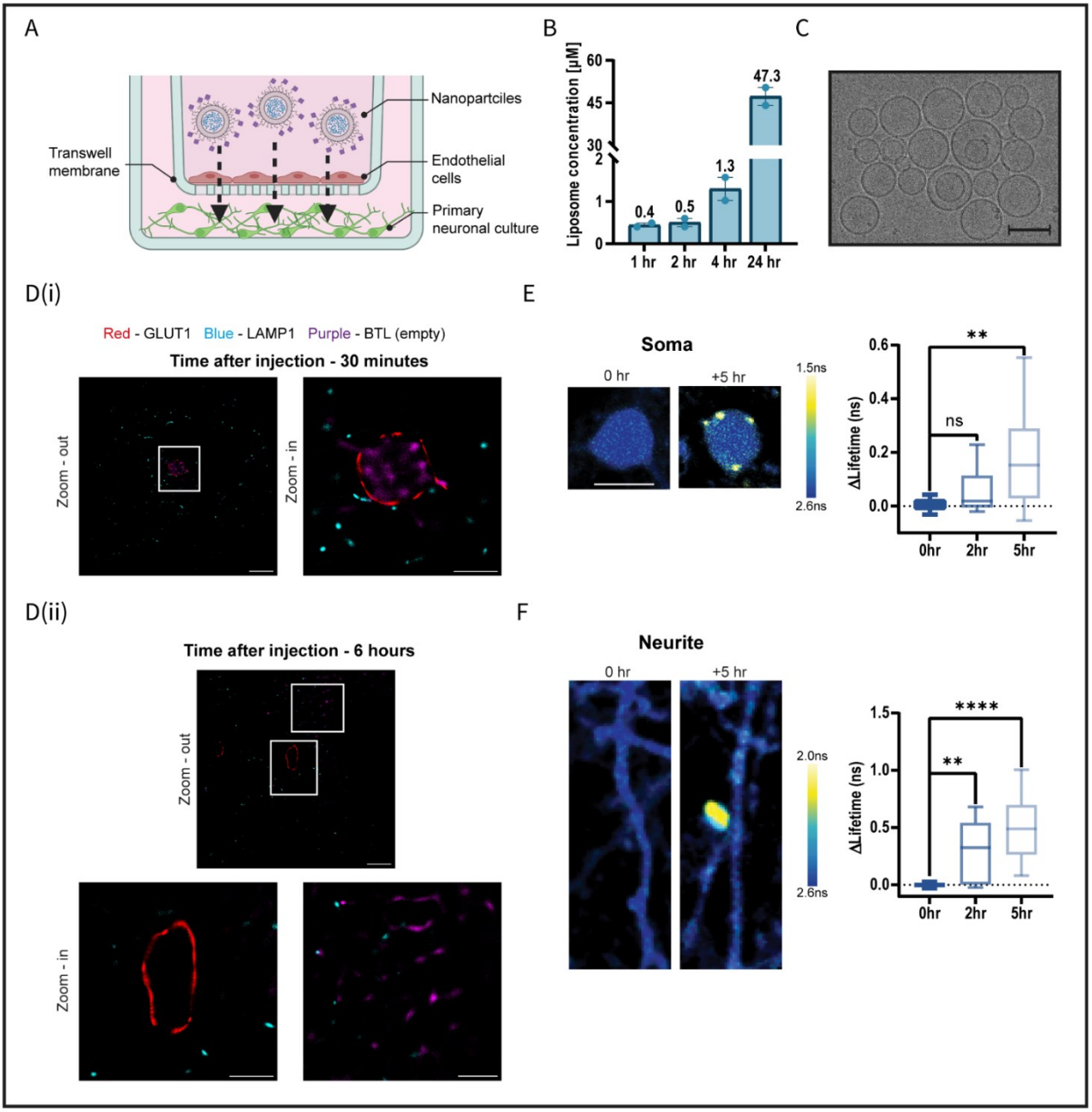

Figure 2. BTL cross the BBB. (A). Schematic illustration of the penetration of BTL (empty) across an *in-vitro* BBB model composed of a co-culture of BMECs atop primary neurons placed in a noncontact manner in a Transwell. **(B).** Concentration in the neurons of the BBB model over time of Cy5-labeled BTL (empty) administrated to the monolayer of BMEC cells, determined by fluorescent measurement. The particle concentration increases over time, reaching 47.3±3.2 ug/ml after 24 hours. **(C).** A Cryo-TEM image showing the liposomes remain intact after crossing (scale bar: 100 nm). **(D).** Tissue dSTORM images of BTL crossing of the BBB: (i) short time after injection and (ii) long time after injection. The liposomes were labeled with AZDye 647 (purple), the capillaries with Alexa Fluor 488 (GLUT1; red), and lysosome molecules with CF568 (LAMP1; blue) (scale bars: zoom-out images 5 um, zoom-in images 2 um). Representative 2pFLIM pseudo-colored images and comparison analysis of the alteration in fluorescence lifetime of **(E)** soma and **(F)** neurite processes 0hr, 2hr, and +5hr after BTL injection, respectively. The liposomes were labeled with Cy3 (yellow), and the cells with GFP (blue) (scale bars: soma images 10 um, neurite images 5 um). The results of B (1 independent repetition performed in 2 replicates), E (13-29 independent repetitions performed), and F (11-26 independent repetitions performed) are presented as mean±SD. One-way ANOVA with adjusted *p*-value in multiple comparison tests was used for the statistical analysis; $^{**}p \leq 0.0012$, $^{****}p < 0.0001$.

Delivery of mAb to neurons

We compared the neuronal uptake and activity of BTL loaded with SynO4 versus free SynO4. Using confocal microscopy, we observed that primary murine cortical neurons overexpressing human alpha-synuclein-A53T, incubated overnight with BTL, had BTL inside the cell body and along the exons (**Figures S13, 3A, and 3B**). Inside the neurons, SynO4 mAbs were released from the liposome and engaged with the target AS aggregates. Only a weak cellular signal was detected in the free SynO4 antibody control group, suggesting the free antibodies did not enter neurons efficiently (p<0.0001) (**Figure 3C**).

Flow cytometry of alpha-synuclein-A53T-overexpressing differentiated human SH-SY5Y (i.e., PD-induced cells) incubated overnight with BTL or free SynO4 demonstrated that 63.4%±2.8% of the cells treated with BTL were positive for SynO4, compared to 2.8%±2.0% of cells treated with free SynO4 (p<0.0001).

In addition, we assessed BTLs' uptake and target engagement using differentiated human SH-SY5Y cells seeded with exogenous AS aggregates. Super-resolution microscopy of the cells after an overnight treatment demonstrated the accumulation of BTL in both neuronal cell bodies and fibers (**Figure S14a and b**). Twelve hours post incubation, 26%±8% of the SynO4 antibody was released from the BTL inside cells, resulting in colocalization and target engagement with 73%±7% of the intracellular AS aggregates (**Figure S14c and d**). Our findings demonstrate the effective intracellular delivery of mAbs using BTL. Inside the neurons, mAbs are released from the liposomes and bound to their target (**Figure S15**).

To test the efficacy of the BTL in reducing AS aggregation and improving neuronal viability, alpha-synuclein-A53T-overexpressing primary murine cortical neurons (PD-induced cells) were treated with either the BTL or free SynO4. After staining for phosphorylated alpha-synuclein, the cells were visualized using dSTORM microscopy (**Figures 3D and S16**), and the number of AS aggregates was analyzed (**Figure 3E**). PD-induced cells treated with BTL exhibited reduced AS aggregation compared to untreated PD-induced cells (p=0.0003) and to PD-induced cells treated with free SynO4 mAbs (p<0.0001). Furthermore, treatment with BTL reverted the cell phenotype to a healthy basal level of AS expression and aggregation. In contrast, the free SynO4 mAb treatment did not reduce the number of AS aggregates.

Next, we treated alpha-synuclein-A53T-overexpressing differentiated human SH-SY5Y (i.e., PD-induced cells) with BTL or free SynO4 and tested their viability (**Figure 3F**). BTL-treated cells exhibited a 76%±2% reduction in the level of late apoptotic/necrotic cells compared to untreated PD-induced cells (p<0.0001) (**Figure 3G**). A negligible decrease in cell death was observed in neurons treated with free SynO4 (p=0.0346), reflecting the low cellular uptake of the mAbs. In addition, the empty BTL (without SynO4) treatment did not significantly reduce

the number of apoptotic cells, indicating the therapeutic effect was primarily due to the SynO4 mAbs loaded into BTL.

These *in-vitro* findings underscore the potential therapeutic efficiency of BTL to reduce AS aggregation and inhibit neuron cell death.

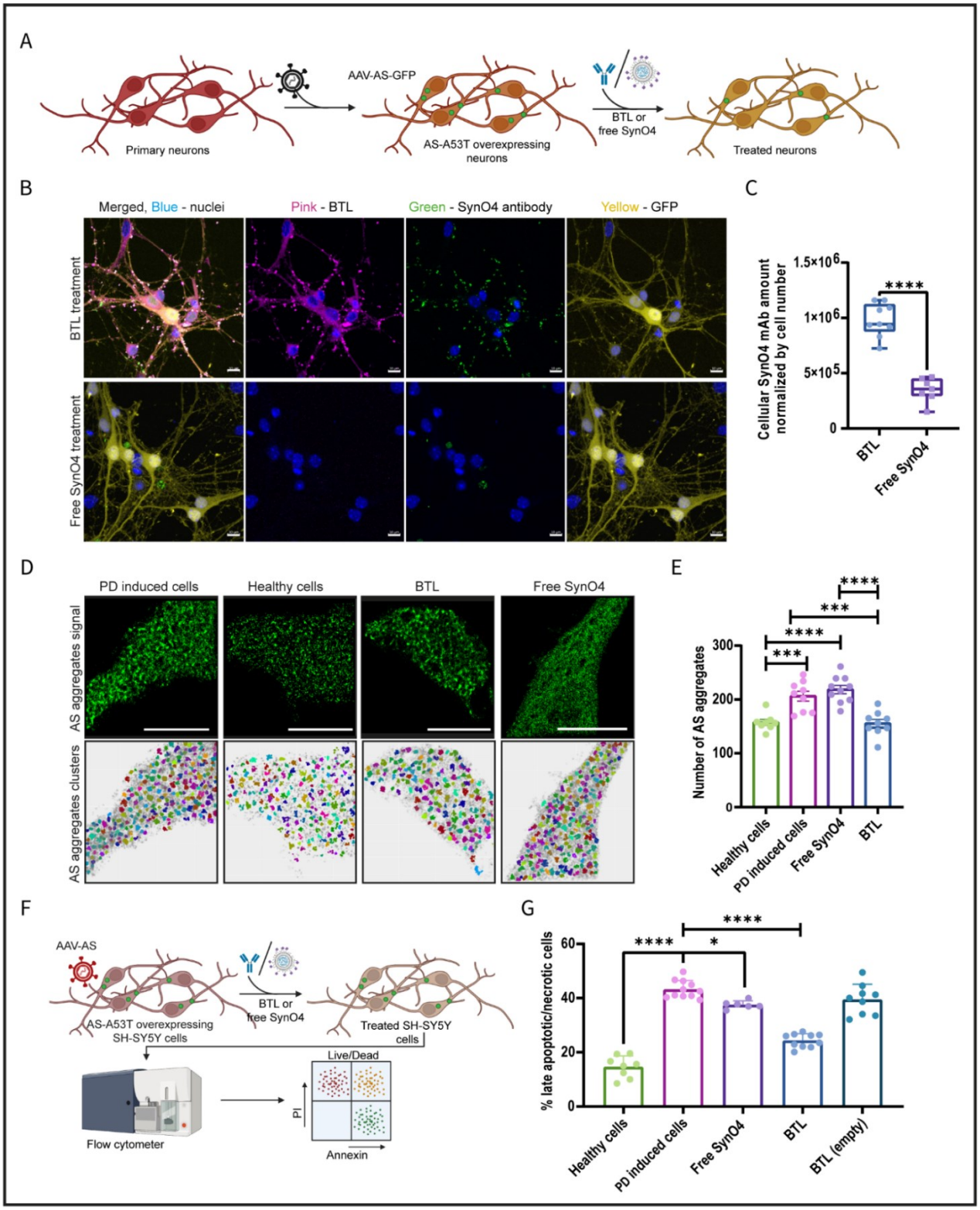

Figure 3. BTL are taken up by PD neurons and induce a therapeutic effect. (A). Schematic illustration of how PD primary neuron cells were infected with a viral vector overexpressing A535 alpha-synuclein and then treated with BTL or with free SynO4 mAbs. **(B).** Confocal images of the uptake of BTL or free SynO4 mAbs in infected PD neurons after overnight incubation. The liposomes were labeled with Cy5 (pink), the antibody with Cy3 (green), and the PD primary neuron cells with GFP (yellow) (scale bar: 10 um). **(C).** Analysis of the cellular SynO4 mAb amount normalized to cell number by IMARIS imaging software. **(D).** dSTORM images of PD-infected neurons treated overnight with BTL or free SynO4 mAbs; the neurons

were marked with GFP (green) (scale bar: 9 um). **(E).** Analysis of the number of AS aggregates using the HDCSCAN algorithm. **(F).** Schematic illustration of PD SH-SY5Y cells infected with a viral vector overexpressing A535 alpha-synuclein, treated with BTL or with free SynO4 mAbs and labeled with Annexin and PI dyes for a live/dead cell viability assay. **(G).** FACS analysis quantification of the percentage of late apoptotic/necrotic cells following the five different treatments. The results of C (3 independent repetitions performed; at least 6 images and at least 60 cells per image), and E and G (3 independent repetitions performed in at least 8 replicates each) are presented as mean±SD. One-way ANOVA with adjusted *p*-value in multiple comparison tests was used for the statistical analysis; **p*=0.0346, ****p*=0.0003, *****p*<0.0001.

BTL accumulate in the brain of PD mice

Overexpression of the TF receptor on the BBB endothelia is a pathological hallmark of PD.[28] As our BTL were designed to target the TF receptor, we first validated that TF receptor overexpression exists also in viral PD-induced mice model. To overexpress AS, C57BC/6JRccHsd male mice were inoculated in the right brain hemisphere substantia nigra with an adeno-associated virus encoding for human alpha-synuclein (AAV2/6-hSyn1-Human SNCA-WPRE-polyA) (**Figure S17**). We found that the relative expression of TfR1 in the brains of AAV-inoculated PD mice was 3-fold higher compared to healthy brains (*p*<0.0005) (**Figure 4A**).

Next, we intravenously injected Cy5-labeled BTL (empty) or Cy5-labeled untargeted liposomes and examined, 12 hours later, their levels in the PD brain (intracellular plus extracellular) and other organs (**Figures 4B, C, and S18**). The accumulation of intravenously administered BTL in PD brains was 3-fold higher than that of the untargeted liposomes (*p*=0.1061), supporting the hypothesis that TF improves BBB penetration and brain targeting (**Figure 4C**). Interestingly, the accumulation of BTL was ~2-fold higher in PD brains than in healthy brain tissue (*p*=0.08533).

In a complementary study, we assessed whether the BTL treatment increases the levels of the mAbs in the brain. PD mice were intravenously injected either with BTL or with free SynO4 mAbs and the brains were processed for antibody quantification in the brain tissue (both intracellular and extracellular) via a direct ELISA assay. Brain tissue following a BTL injection had 2.3-fold more antibodies than brain tissue following a free SynO4 injection (*p*<0.05) (**Figure 4D**). We also evaluated the accumulation of intracellular liposomes in the brain following the intravenous injection of Cy5-labeled BTL loaded with Cy3-labeled SynO4 or of free Cy3-labeled SynO4, by way of confocal microscopy of frozen brain sections (**Figure S19**). Our findings confirm that the encapsulation of SynO4 mAbs in targeted liposomes enhances brain delivery both to the brain parenchyma and to brain cells.

To assess the magnitude of nanoparticle delivery versus free antibody delivery at the cellular level, PD mice were injected intravenously with Cy5-labeled components: BTL (empty), free SynO4 or transferrin-targeted-SynO4 (i.e., SynO4 with TF conjugated directly to the mAb). Post-intravenous administration brains were digested for single-cell analysis, and Cy5-positive cells were recorded (**Figure 4E**). A quantitative FACS analysis 12 hours after injection

demonstrated that the total number of Cy5-positive cells in the PD brains was 5.4-fold higher than in healthy mouse brains (p<0.005) (**Figure 4F**). The number of Cy5-positive cells observed following BTL delivery was 7.6-fold greater than following free antibody delivery (p<0.005) and 1.6-fold greater than following targeted free SynO4 delivery (p<0.00181).

We also analyzed the distribution of BTL in the different cell populations in PD and healthy brains. To do so, brain cells were labeled using an antibody panel for microglia (CD45+, CD11b+), endothelial cells (CD31+), astrocytes (CD44+), and neurons (CD24+; **Figures S20 and S21**). In the PD brains, 35%±11% of the endothelial cells were positive for BTL (**Figure 4G(i)**), whereas only 8%±2% were positive in healthy brains (**Figure 4G(ii)**). As to the neurons in PD brains, 12%±1% of the neurons in PD brains were positive for BTL (**Figure 4G(i)**), in comparison to 8%±2% in healthy brains [29] (**Figure 4G(ii)**). Lower liposomal uptake was detected in microglia and astrocytes of PD and healthy mice (**Figure 4G**).

PD is characterized by the death of dopaminergic neurons in the brain. We measured the uptake of BTL by dopaminergic neurons in comparison to other neuronal subtypes.[2, 30] For this, PD mice were intravenously administered with BTL, their brains were resected, and the brain cells were labeled with specific markers for microglia, endothelial cells, astrocytes (as detailed above), as well as dopaminergic neurons (Dopamine Transporter+) (**Figure S22a**). The mean fluorescent intensity (MFI) of Cy5-labeled BTL inside dopaminergic cells was 6222±2154, ~1.9-fold higher than the MFI of 3200±1514 in other neuronal subtypes or oligodendrocytes. Similar results were also obtained for the SynO4 content in the dopaminergic neurons. Intravenous BTL administration led to a higher MFI of Cy3-labeled SynO4 mAbs (17,840±9737, ~2.3-fold) inside dopaminergic neurons compared to 7835±5669 intensity in other neuronal subtypes or oligodendrocytes (**Figure S22b and c**). The higher uptake of the BTL in dopaminergic neurons can be explained by the over-expression of TF receptors on these cells during PD.[31]

To assess the internalization of BTL within dopaminergic neurons, we used confocal microscopy to visualize patient-derived dopaminergic neurons having amplified copies of the SNCA gene.[32] After incubation, BTL were detected inside the cytoplasm and along the exons of the patient-derived PD neurons (**Figure 4H**).

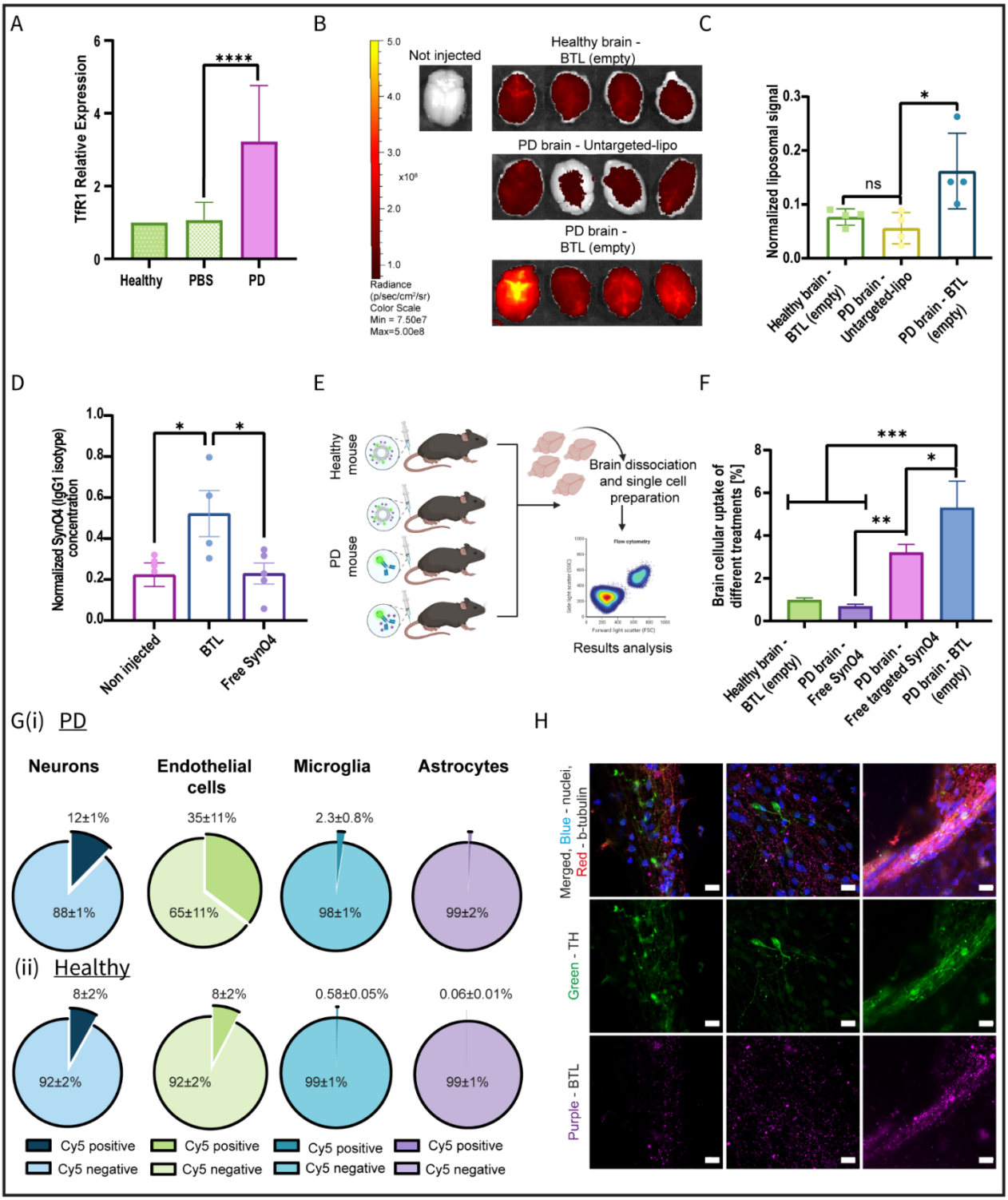

Figure 4. BTL cross the BBB and accumulate significantly in PD mice brains. (A). RT-PCR analysis of the levels of TfR1 receptors in the PD brain; the TfR1 expression levels were normalized to the healthy group and were obtained according to the $2^{-\Delta\Delta Ct}$. **(B-C).** The nanoparticle biodistribution in the brains of PD-induced and healthy mice 12 hr after the administration of Cy5-labeled BTL (empty) or Cy5-labeled untargeted-liposomes, analyzed using an in-vivo imaging system (IVIS) (B) and quantified by IVIS software analysis (C). **(D).** The level of the IgG1 isotype (SynO4 isotype) in PD brains following liposome delivery or antibody delivery, was determined using an ELISA assay. **(E).** Schematic illustration of the flow cytometry setup experiment. **(F).** The levels of BTL (empty), transferrin-SynO4 mAb, and free SynO4 mAb in PD brain cells and those of BTL in healthy brains, were determined using flow-cytometry. **(G).** Quantification of the cellular uptake of BTL in neurons,

endothelial cells, microglia, and astrocytes in (i) PD brains and (ii) healthy brains. **(H).** Confocal imaging of the cellular uptake of BTL in human PD dopaminergic neurons. The liposomes were labeled with Cy5 (purple), and the cells were stained with tyrosine hydroxylase (TH, green), b-tubulin (red), and nuclei (blue) (scale bar: 10 um). Results of A, C, and E (5 independent repetitions) and D and F (4 independent repetitions) are presented as mean±SD. One-way ANOVA with an adjusted *p*-value in multiple comparison tests was used for statistical analysis in A, C, D, and F; *$p \leq 0.1061$, ***$p \leq 0.0002$, ****$p < 0.0001$.

BTL reduce AS aggregation and neuroinflammation in AAV-inoculated PD mice

To examine the ability of BTL to reduce AS aggregation in the brain, AAV-inoculated mice overexpressing AS (PD-induced) were treated with either free SynO4, BTL or not treated (disease control), with a healthy group used as a second control. Each group was injected intravenously every other day for two weeks or four weeks (**Figure 5A**). AS levels, neuron survival, and the levels of activated microglia and reactive astrocytes in the substantia nigra were assessed using immunohistochemistry. AS aggregates were labeled using a 5G4 antibody, whereas the number of dopaminergic neurons was detected using a tyrosine hydroxylase (TH) antibody, which recognizes TH enzyme expression by dopaminergic neurons (**Figures 5B(i), C(i), S23, and S24**).

To study neuroinflammation[33], activated microglia cells were detected using the ionized calcium-binding adaptor molecule 1 (Iba1) antibody (**Figure S25**). In addition, the number of reactive astrocytes was calculated using the glial fibrillary acidic protein (GFAP) antibody, which is expressed exclusively in astrocytes (**Figure S26**).

Two weeks after the treatment began, the percentage of extracellular AS aggregates decreased significantly in the BTL-treated group (76%±12% reduction) compared to the free antibody antibody-treated group (45%±10% reduction) (p=0.0004) (**Figure 5B(ii)**). Analyzing the number of cells exhibiting aggregated AS and the total amount of aggregated AS (extra- and intra- cellular), showed that the BTL treatment resulted in lower levels of AS-positive cells (~2.8-fold, p=0.0006) as well as total AS accumulation (~2.5-fold, p=0.0005), compared to untreated PD mice (**Figure S27a and b**).

We next evaluated the percentage of live dopaminergic neurons by comparing the number of neurons on the inoculated side (right hemisphere) with those on the non-infected side (left hemisphere). A 2-week viral PD-induced injection resulted in a 24%±12% reduction in dopaminergic neurons without any treatment (p=0.0026) (**Figure 5B(iii)**). Some improvement in the survival of dopaminergic neurons was recorded in the BTL group (81%±9% survival vs. 76%±12%-healthy: p=0.0147) compared to the free SynO4 treatment (73%±12% survival vs. 76%±12%-healthy: p=0.0002).

As the reactive glia process involves molecular and morphological changes in astrocytes and microglia cells, including increased expression of GFAP[34] and Iba1[35] markers, respectively, we assessed these biomarkers in the mice 2-week post viral PD-induced injection. We found that both the BTL and free antibody administrations led to a reduction in activated glial cells

compared to the PD untreated group (p<0.0001) (**Figure 5D(i) and D(ii)**). However, the reduction in the activated microglia cells was more significant following the BTL treatment (~3.4-fold, p<0.0001) compared to the free SynO4 treatment (~1.7-fold, p=0.0032) (**Figure 5D(i)**).

Four weeks after the BTL treatment, the percentage of extracellular AS aggregates decreased further (69%±9% reduction) compared to 50%±10% reduction in mice treated with the free SynO4 mAbs (p=0.0198) (**Figure 5C(ii)**). Furthermore, compared to the PD untreated group, the number of AS-positive cells in the BTL-treated group decreased by ~1.5-fold (p=0.0097) (**Figure S27c**), and the total amount of AS aggregates reduced by ~3-fold (p<0.0001) (**Figure S27d**).

In summary, BTL treatments reduced AS aggregation compared to free SynO4 and other controls.

Four weeks after viral AS inoculation, the survival of dopaminergic neurons in the PD untreated group was 60%±11% (**Figure 5C(iii)**). The BTL treatment slowed down the loss of dopaminergic neurons, resulting in a neuronal survival rate of 70%±10%, whereas free antibody treatment achieved only 53%±26%, thereby demonstrating a trend of dopaminergic neuron survival. The glial inflammation continued to progress, after four weeks following the viral PD-induced injection (**Figure 5E(i) and E(ii)**). A significant reduction in the number of activated microglia cells was observed in the PD mice treated with either BTL or free SynO4 (p<0.0001) (**Figure 5E(i)**). In the BTL-treated group, the reduction in the number of inflammatory astrocytes was far more pronounced than in the PD-untreated group (p=0.0363); the free antibody treatment did not show any signs of reduction (p=0.9375) (**Figure 5E(ii)**).

Taken together, our findings indicate that the brain-targeted liposomes loaded with SynO4 mAbs (BTL) reduce AS aggregation and neuroinflammation, thereby slowing neuronal degeneration. All of the tested parameters indicate that the liposomal intravenous administration has greater efficacy than free antibody intravenous administration, demonstrating the ability of this brain-targeted delivery system to overcome the challenges of brain biological therapies, including crossing the BBB, penetrating cell membranes, and contributing to neuroprotection.

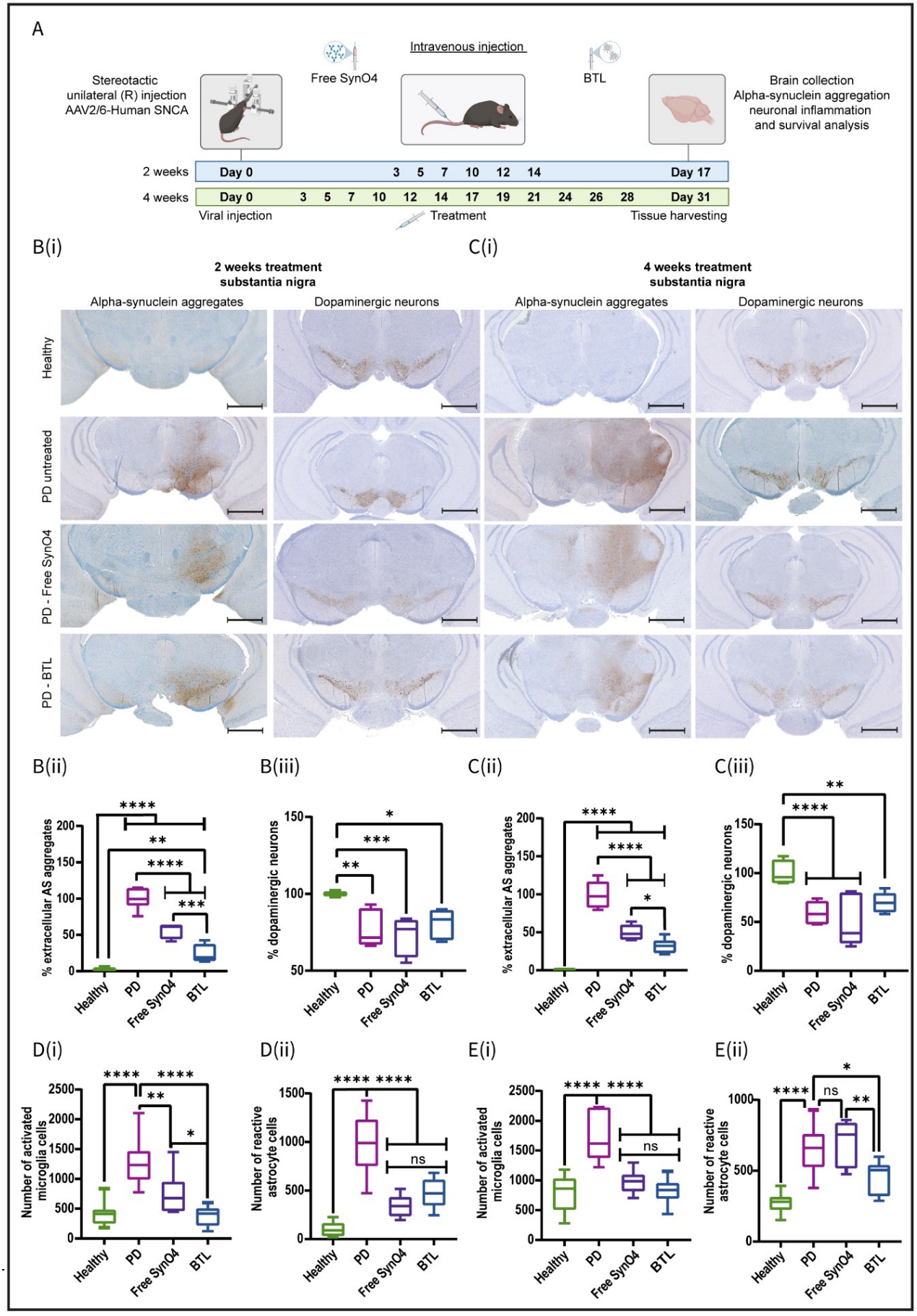

of the therapeutic efficacy experiment: Healthy mice received unilateral AAV injection encoding human AS at the right side of the brain. Then, the mice were injected every other day with the different treatments, i.e., free SynO4 mAbs or BTL for 2 or 4 weeks. In the final stage, the brains were harvested, cut into sections, and stained for biochemical and histological analysis and compared with the untreated PD group and the healthy group **(B(i), C(i)).** Representative images of histological brain sections of the substantia nigra area after (B(i)) two weeks and (B(ii)) four weeks of treatment. Sections were stained against aggregated AS and dopaminergic neurons (scale bar: 2000 um). **(B(ii), C(ii)).** The percentage of aggregated AS in the different treatments after (B(ii)) two weeks and (C(ii)) four weeks of treatment. **(B(iii), C(iii)).** The percentage of dopaminergic neuron survival after (B(iii)) two weeks and (C(iii)) four weeks of treatment. The healthy group values were normalized to 100%, and the other group's values were normalized to the mean value of the healthy group. **(D(i), E(i)).** The number of activated microglia cells (D(i)) after two weeks and (E(i)) four weeks of treatment; the cuts were stained against the Iba1 marker. **(D(ii), E(ii)).** The number of reactive astrocyte cells (D(ii)) after two weeks and (E(ii)) four weeks of treatment; cuts were stained against GFAP marker. The results of B(ii), B(iii), D(i), D(ii) and E(ii) (3-4 independent repetitions in 1-3 technical replicates), C(iii) and E(i) (4-5 independent repetitions in 1-3 technical replicates) and C(iii) (3-5 independent repetitions in 1-3 technical replicates) are presented as mean±SD. One-way ANOVA was used for the statistical analysis in B, C, D, and E; *p≤0.0370, **p≤0.0072, ***p≤ 0.0004, ****p< 0.0001.

BTL improve motor function and motor learning in PD mice

We examined the effect of BTL treatments on motor function and motor learning (**Figures 6 and S28**). AAV-inoculated mice overexpressing AS were divided randomly into four groups: PD untreated, PD treated with free SynO4 mAbs, and PD treated with BTL; healthy mice were used as a control group. Treatment groups were injected with an intravenous injection every other day for 4 weeks and examined in a rotarod after 2 and 4 weeks of treatment (**Figure 6A**). Two weeks after the treatment, the BTL group achieved similar motor function outcomes to the healthy control group (p<0.7607) (**Figure 6B**). On the other hand, mice receiving free SynO4 mAbs had a reduced latency to fall compared to the BTL group (p<0.0074). Additionally, we evaluated the short-term motor learning capacity of the mice (**Figure 6C**). Both healthy and BTL groups were able to improve their performance along the days increasing their latency to fall (Healthy and BTL Day 1 vs. Day 3: p<0.0001). Free SynO4 and untreated-PD groups showed reduced motor learning, maintaining a stable performance capacity (PD Day 1 vs. Day 3: p<0.0497; free SynO4 Day 1 vs. Day 3: p<0.0138). On the third day of measurement, a significant difference was observed between the BTL group and PD untreated group (p<0.0067) and the free SynO4 group (p<0.0025).

After 4 weeks of treatment, the mice were measured in the rotarod to determine the long-term motor learning capacity (**Figure 6D and E**). A 2-fold improvement in performance was observed in healthy and BTL groups on the third day of measurement (the end point of motor learning) compared to the beginning of the experiment (**Figure 6D**). PD untreated and free SynO4 had shorter latency to fall, compared to healthy control (p<0.0042 and p<0.0106, respectively) while in the case of BTL, the difference was not significant compared to the healthy group (p=0.4636). Free SynO4 achieved values comparable to PD untreated mice (p=0.9906), while BTL improved the performance (p=0.2047). The PD untreated group showed no significant improvement from the first day of motor functioning to the last day of motor learning (**Figure 6E**).

This behavioral study demonstrates the promise of BTL in improving motor function and learning abilities in virally inoculated PD mice (**Movie S3**).

Preliminary safety of BTL in mice

After 40 days of treatment, blood samples were taken to evaluate the safety profile of BTL. Representative histopathological organ sections were analyzed from the liver (**Figure 6F(i)**), kidney (**Figure 6G(i)**), and spleen (**Figure 6H(i)**). The tissue was stained with hematoxylin and eosin to identify cell structure. No apparent differences were found between the healthy and BTL groups in any of the organs. Specifically, no steatosis and no peri-portal or parenchymal inflammation were seen in the liver. The glomerular and tubular structures were normal, with no interstitial inflammation.

To evaluate potential hepatotoxicity (**Figure 6F(ii)**), hepatic enzymes including aspartate transaminase (AST) (**Figure S29a**), alanine transaminase (ALT) (**Figure S29b**), lactate dehydrogenase (LDH) (**Figure S29c**), alkaline phosphatase (ALP) (**Figure S29d**), and total bilirubin (T.Bil) (**Figure S29e**) were measured. No significant differences were detected between the healthy and BTL groups. A slight increase in hepatic enzyme levels and bilirubin levels was observed following free SynO4 administration (**Figures 6F(ii), S29a, and e**).[36] Nephrotoxicity (**Figure G(ii)**) was evaluated by measuring creatinine (**Figure S29f**), urea (**Figure S29g**), and albumin (**Figure S29h**) levels in the blood. No differences were appreciated between the healthy and BTL groups. Blood cell levels (**Figure 6H(ii)**) were determined by measuring %lymphocytes (**Figure S29i**), %neutrophils (**Figure S29j**), lymphocyte antibodies (**Figure S29k**), and neutrophile antibodies (**Figure S29l**). PD, free SynO4, and BTL groups showed higher levels of white blood cells (WBC) (**Figure 6H(ii)**), as well as lymphocytic antibodies (**Figure S29k**), all of which may have been influenced by the increased amounts of AS that induced inflammation and an immune response.[37] However, the free SynO4 treatment resulted in a reduction in neutrophil levels (neutropenia, **Figure S29j**).

These data show that the administration of the BTL over a period of 4 weeks was favorably tolerated and did not cause organ toxicity.

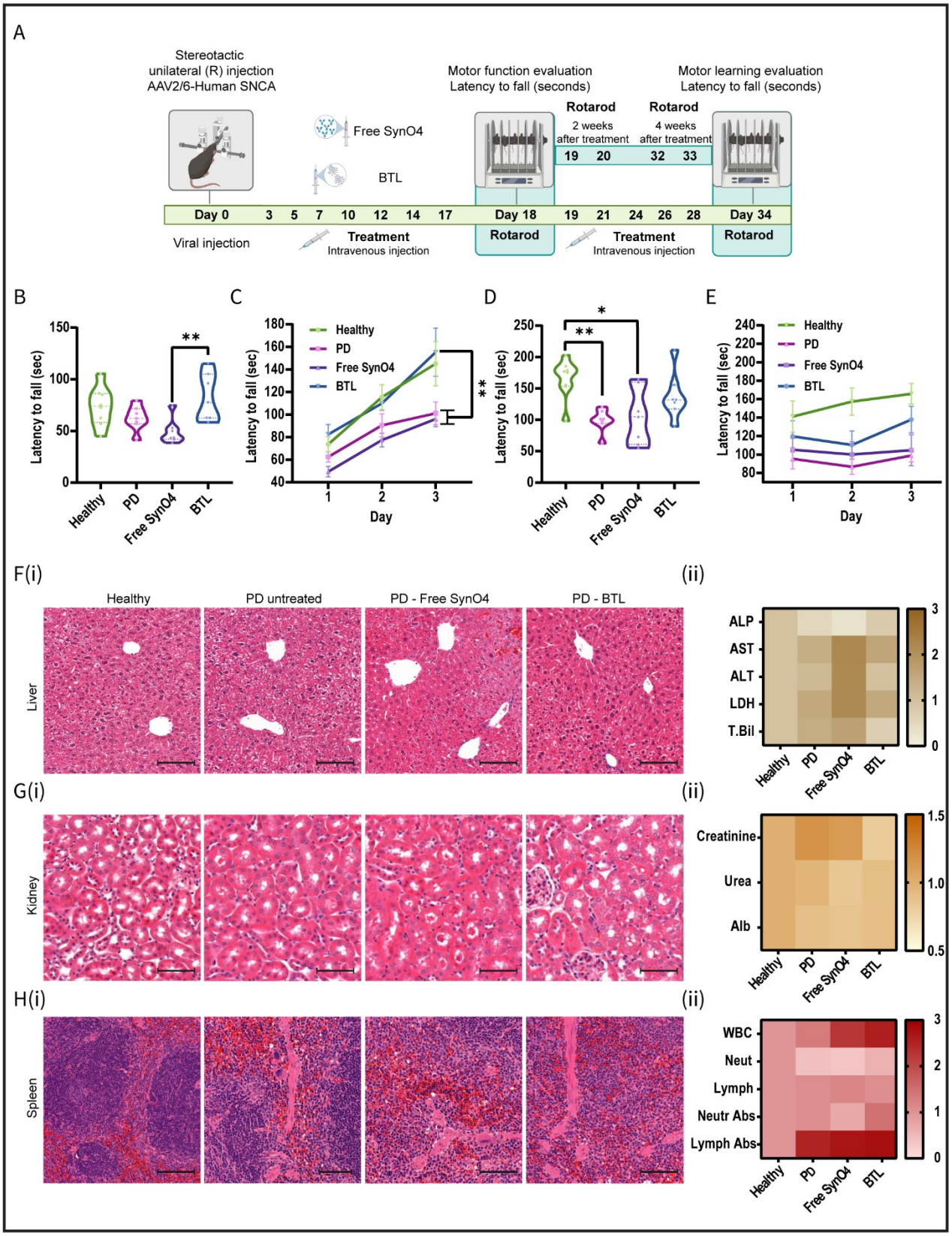

Figure 6. The capacity of BTL to prevent disease progression in a viral PD mice model. (A). Illustration of the behavioral therapeutic efficacy experiment: Healthy mice received a unilateral AAV injection encoding human AS. Then, the mice were injected every other day with either free SynO4 or BTL for 2 or 4 weeks. At the end of the treatment period, the mice were

measured on 3 consecutive days in an accelerating speed rotarod to detect coordination and balance functions. **(B).** Motor functioning capacity on the first day of rotarod evaluation after 2 weeks of treatment. **(C).** Short-term motor learning capability after 2 weeks of treatment. **(D).** Motor functioning capacity on the last day (day 3) of rotarod evaluation after 4 weeks of treatment. **(E).** Long-term motor learning after 4 weeks of treatment. **(F).** Histological organ sections (i) liver, (ii) kidney, and (iii) spleen on day 40 of the experiment. Sections were stained with hematoxylin and eosin to identify the cell's structure. No differences in cell structure were found between healthy and BTL groups in all the evaluated organs (scale bar: 100 um). **(F(i)).** Hepatotoxicity test of blood on day 40 of the experiment. Hepatic enzymes, Alkaline phosphatase (ALP), Aspartate transaminase (AST), Alanine transaminase (ALT), Lactate dehydrogenase (LDH), and total bilirubin (T.Bill) were measured. No differences were detected between the healthy and BTL groups. The presence of free Syno4 resulted in increased levels of hepatic enzymes as well as bilirubin, indicating liver damage. **(G(ii)).** Nephrotoxicity test of blood on day 40 of the experiment. Creatinine, urea, and albumin levels were measured. No differences were detected between the healthy and BTL groups. **(H(ii)).** White blood cell count (WBC) test of blood was collected on day 40 of the experiment. No differences were found between the healthy and BTL groups. All values are normalized to the healthy group's values. Neut- Neutrophils, Lymph- Lymphocytes. The results of F are representative sections of 3 independent repetitions performed in 1-3 technical replicates. The results of B and D (7-8 independent repetitions) are presented as mean±SD. One-way ANOVA was used for statistical analysis; *p≤0.0109 **p≤0.0049. Results of C and E (7-8 independent repetitions) are presented as mean±SD. Two-way ANOVA was used for statistical analysis; *p≤0.0106 **p≤0.0075.

Conclusion

We engineered transferrin-targeted liposomes loaded with SynO4 (BTL) to treat PD. The synthetic approach involved loading SynO4 monoclonal antibodies into 100-nm liposomes and then conjugating a targeting moiety (TF) to their outer surface via covalent bonds. SynO4 was shown by us and others to bind and inhibit AS aggregation, however, its brain penetration is inferior in its free, non-liposomal, form.

To preserve the bioactivity and integrity of SynO4 during the formulation process, DPPC, a phospholipid with a favorable phase transition temperature (Tm=41ºC) was selected as the main lipid component of the nanoparticles. BTL have 95±23 TF units on their outer surface, encapsulate 33±6 SynO4, and were shown to remain stable for 2 weeks when preserved at 4°C.

In vitro, BTL crossed BMEC endothelial BBB monolayers, escaping endocytic pathways and retaining their structural and functional integrity.

BTL were taken up readily by patient-derived neurons and primary cortical neurons, distributed throughout the cell body and axons. Inside the neurons, SynO4 was released, binding its AS target, resulting in reduced AS aggregation and increased neuronal viability. Free SynO4 did not penetrate neurons efficiently.

In vivo, intravenously administered BTL accumulated favorably in the brain of PD mice, compared to untargeted liposomes or free SynO4 administrations.

The accumulation of nanoparticles was primarily observed in brain endothelial cells. A contributing factor to this result is that endothelial cells are the first point of contact for circulating BTL as they cross the BBB.[12] Another contributing factor is endothelial cells' overexpression of TF receptors in the brain's microvasculature, which enhances the uptake of BTL through receptor-mediated transcytosis.[17a] In addition to endothelial cells, dopaminergic

neurons are also responsible for the uptake of a significant amount of BTL in the brain.[17b, 38] The overexpression of TF receptors in neurons during PD enables the selective accumulation of the nanoparticles in these cells after they cross the BBB.[29]

Recent *in vitro* and *in-vivo* studies suggest that liposomal uptake by neurons can be enhanced by PEG molecules on their surface.[23] The length of the PEG chain extending from the liposome surface plays an important role in cellular uptake and targeting capacity. Our findings indicate that conjugating TF moieties to a long PEG2000 chain, while the remainder of the steric PEG molecules are PEG1000, results in superior uptake by brain endothelial cells. This result is attributed to the steric effect of neighboring PEG molecules on the formulation that if too long, disguises the TF targeting moiety from its biological target.

Most importantly, we show that BTL slow down the progression of Parkinson's disease in mice. BTL were found to reduce AS aggregation and cell death in PD neurons compared to free SynO4. Intravenous injection of BTL to PD mice significantly reduced AS aggregation and neuroinflammation after 2 and 4 weeks of treatments, both intracellularly and extracellularly.
Additionally, BTL treatments improved motor function and motor learning capabilities, with a favorable safety profile.
To summarize, this study demonstrates that targeted nanoparticles cross the BBB and deliver antibodies intracellularly and extracellularly to the brain during Parkinson's disease, supporting this approach's utility for treating additional neurodegenerative diseases.

Experimental Section

ELISA establishment

An in-house ELISA assay using the direct ELISA method was developed for the Anti-Human SNCA Therapeutic (SynO4) Antibody (Creative Biolabs, USA, TAB-0750CLV-L) (**Figure S2**). A 384-well plate was coated with 1.4 ug/ml Recombinant Human Alpha-Synuclein Protein Aggregates Active (Abcam, UK, ab218819), sealed, and incubated overnight at 4ºC. The next day, blocking (5% Fetal Bovine Serum (FBS; Rhenium, Israel, K210430) in PBST (Dulbecco's Phosphate Buffered Saline (PBS; Sigma-Aldrich, Israel, D8537) with 0.05% Tween20 (Sigma-Aldrich, Israel, P1379))) was performed, followed by the addition of known concentrations of SynO4 antibody. Next, the PBST was washed out and the plate was incubated with a dilution of 1/100,000 of secondary antibody (Goat Polyclonal to Mouse IgG1-HRP, Abcam, UK, ab6789). TMB ELISA Substrate (Abcam, UK, ab171522) was used for signal development, which was detected by kinetics absorbance measurement using a plate reader (reading at 650 nm with two minutes intervals for an hour). A linear calibration curve for the SynO4 antibody (**Figure S1b**) was generated based on the described ELISA setup. For the generation of the

standard IC50 curve (**Figure S1c**), SynO4 was pre-incubated with a 10-fold serial dilution of AS aggregates.

To determine the working temperature for the nanoparticle preparation with the SynO4 antibody, the antibody samples were pre-heated at different temperatures (35ºC, 45ºC, 55ºC, and 65ºC) for 1 hour; a non-heated antibody sample (25ºC) was also used. The samples were either kept first overnight at 4ºC or were immediately incubated with known concentrations of AS aggregates to generate IC50 curves (**Figure S1f and S1d**, respectively) and graphs of the maximum antibody activity percentage (**Figure S1g and S1e**, respectively).

BTL fabrication

The liposomes' fabrication was performed using the thin-film method. First, 100mM of total lipid mixture of DPPC (Lipoid, Germany, 556610), cholesterol (Sigma-Aldrich, Israel, C8667), 1,2-distearoyl-sn-glycero-3-phosphoethanolamine-N-[methoxy(polyethylene glycol)-1000] (ammonium salt) (DSPE-PEG1000) (Biopharma PEG, USA, 001096) and 1,2-distearoyl-sn-glycero-3-phosphoethanolamine-N-[amino(polyethylene glycol)-2000] (ammonium salt) (DSPE-PEG2000-NH2) (Biopharma PEG, USA, 10455) in molar percentages of 60:30:2.5:2.5 was dissolved in chloroform. For the preparation of untargeted liposomes, 1,2-distearoyl-sn-glycero-3-phosphoethanolamine-N-[methoxy(polyethylene glycol)-2000] (ammonium salt) (DSPE-PEG2000) (Lipoid, Germany, 29232000) was used instead of DSPE-PEG2000-NH2.

Then, using a rotary evaporator, the chloroform was evaporated (45°C, 50 rounds per minute (rpm)) to form a thin homogenous lipid film, which was stored in a vacuum at -20°C for further use. Next, the film was hydrated with 2 mg/ml of SynO4 antibody solution in PBS for 1 hour, at 45°C, 50 rpm to create liposomes loaded with SynO4 mAbs; in the case of empty liposomes, the solution contained only PBS. Next, the liposome mixture was extruded through 400-, 200-, 100-, and 80- nm pore-size polycarbonate membranes (LIFEGENE, Israel, 10417106, 110606, 110605, and 110604, respectively), using a LIPEX extruder (Northern Lipids, Canada), at 45°C, with a maximum working pressure of 15 bar, to obtain homogenous 100 nm liposomes. Finally, the non-encapsulated SynO4 antibodies were removed by dialysis against PBS pH 7.4 (1:1000 volume ratio) using a 1000 kDa dialysis membrane (Repligen, USA, 131486) at 4ºC for 48 hours. The buffer was exchanged four times during the 48 hours and the dialysis bag was replaced with a new bag at each change (**Figure S2**).

To quantify the encapsulation concentration of the SynO4 antibody within the liposomes, the liposomes were diluted in several dilutions and incubated in a blocking solution with 0.5% Triton X-100 (Sigma-Aldrich, Israel, 93443) for 1 hour, at 25°C to release the SynO4 antibodies into the supernatant; as positive controls, untargeted liposomes or transferrin-conjugated liposomes without SynO4 mAbs (herein BTL (empty)) were mixed with a known concentration of SynO4. Next, the ELISA steps were performed as described above. Finally, a

linear calibration curve for the SynO4 antibody was obtained using the absorbance values to quantify the concentration of SynO4 inside the liposomes. The SynO4 mAb encapsulated units per liposome were calculated using the calculated SynO4 concentration and the liposome particle concentration as follows:

Equation 1: $C_{mAb} = X\ [ug/ml] \times Y\ [ml] = Z\ [ug]$

Equation 2: $N_{mAb} = C_{mAb}/Mw_{mAb} = Z\ [ug]/\ 150{,}000\ [gr/mole] = Q\ [mole]$

Equation 3: $Units_{mAb} = n_{mAb} \times N = Q\ [mole] \times 6.022\text{^}10^{23} = mAb\ units$

Equation 4: $Units_{liposomes} = L\ [particles/ml] \times Y\ [ml] = Liposomes\ units$

Equation 5: $mAb\ encapsulated\ units\ per\ liposome = Units_{mAb}/Units_{liposomes}$

Transferrin-to-liposome conjugation

Holo-Transferrin Human (Sigma-Aldrich, Israel, T4132) was cross-linked to the surface of the liposomes by N-(3-Dimethylaminopropyl)-N'-ethyl carbodiimide hydrochloride (EDC; Sigma-Aldrich, Israel, 03450) and N-Hydroxysulfosuccinimide sodium salt (Sulfo-NHS) (Tzamal D-Chem Laboratories Ltd, Israel, FH24507) reagents. First, 10 mg/ml of transferrin solution (PBS), 15 mg/ml of Sulfo-NHS (PBS) solution, and 15 mg/ml of EDC solution (DMSO) were prepared. Second, each of the reagent solutions was added to the transferrin solution to reach a 1:25 molar proportion (transferrin: Sulfo-NHS) and 1:10 molar proportion (transferrin: EDC). The pH of the transferrin solution with the reagents was adjusted to 6, with 1.2M HCL. Third, the solution was mixed (450 rpm) at 25°C for 1 hour. Fourth, the transferrin solution was dialyzed against PBS pH 6 (1:1000 volume ratio) using a 12-14 kDa dialysis membrane (Repligen, USA, 132700) at 4ºC overnight, to remove the excess of the regents. Fifth, BTL (empty) were synthesized by mixing 100 nm empty NH2-liposomes (100 mM) with a transferrin solution, and transferrin-conjugated liposomes loaded with SynO4 mAbs (herein BTL nanoparticles) were synthesized by mixing 100 nm NH2-liposomes loaded with SynO4 (100mM) with a transferrin solution, to reach a final liposomal concentration of 50mM and a molar proportion of 10:1 (liposomes: transferrin). Sixth, the pH of the liposomes' reaction was

adjusted to 8.4 with 1M sodium bicarbonate, and the reaction was incubated for 2 hours, at 450 rpm, at 25 ºC. Lastly, the non-conjugated transferrin was removed by dialysis against PBS pH 7.4 (1:1000 volume ratio) using a 1000 kDa dialysis at 4ºC for 48 hours. The buffer was exchanged thrice (after 1 hour, 4 hours, and overnight) for the BTL (empty); for the BTL with SynO4, an additional exchange was performed on the next day, followed by changing to a new bag overnight (**Figure S2**).

The Micro BCA Protein Assay Kit was used to quantify the number of transferrin units on the liposomes' surface (Thermo-Fisher, Rhenium, Israel, 23235). First, a calibration curve of transferrin was prepared. To quantify the number of TF units on the BTL with SynO4/empty, each tube of the calibration curve contained transferrin at a known concentration, with SynO4/empty liposomes (5%, 100mM), and Triton-X100 (2%); the remaining volume was PBS. In addition, the liposome sample was prepared by mixing 10% of BTL with SynO4/empty (50mM) with 2% Triton-X100 in PBS. Afterward, the samples (calibration curve and liposome) were incubated at 58°C for 1 hour and centrifuged (13,000 rpm, 10 min) to burst the liposomes and obtain a clean supernatant. The clean supernatant from each sample was transferred to a 96-well plate. A BCA reagent, prepared according to the manufacturer's instructions, was added to the wells with the samples. The plate was sealed and incubated at 37°C for 1 hour. Then, the plate was cooled down to 25°C (~8 min), and the absorbance values were read at 562 nm using a plate reader (Tecan, Switzerland). A linear calibration curve for transferrin was obtained using the absorbance values to quantify the amount of transferrin (ug/ml) on the liposomes. Then, the number of TF units per liposome surface was calculated using the transferrin concentration and the liposome particle concentration as follows:

Equation 1: $C_{TF} = X\ [ug/ml] \times Y\ [ml] = Z\ [ug]$

Equation 2: $n_{TF} = C_{TF}/Mw_{TF} = Z\ [ug]/\ 76{,}000\ [gr/mole] = Q\ [mole]$

Equation 3: $Units_{TF} = n_{TF} \times N = Q\ [mole] \times 6.022\text{^}10^{23} = TF\ units$

Equation 4: $Units_{liposomes} = L\ [particles/ml] \times Y\ [ml] = Liposomes\ units$

Equation 5: $TF\ units\ per\ liposome\ surface = Units_{TF}/Units_{liposomes}$

Physical liposome characterization

The measurement of liposomes' physical parameters, including mean size diameter [nm], particle size distribution, PDI, and zeta potential [mV], was carried out by dynamic light scattering using a Zetasizer Nano (ZSP, Malvern, UK). The particle concentration [particles/ml] measurements were carried out using a Zetasizer Ultra (Malvern, UK). The drug-loading rate was calculated as follows (**Figure S3**):

Equation 1: C_{SynO4} *[µmole] =* (C_{SynO4} *[ug/ml, Figure 1C and S4] x 1.5 [ml, sample volume]) / 150,000 [gr/mole]*

Equation 2: *(µmole antibody/ µmole lipid)* min^{-1} *=* (C_{SynO4} *[µmole] / 350 [µmole, total amount of lipids in the formulation]) 60* [min^{-1}*, hydration time]*

BTL release profile

BTL and free SynO4 mAbs were dialyzed against PBS 7.4 (1:1000 volume ratio), at 37°C, using a 1000 kDa dialysis membrane, at 60 rpm. For each time interval, the remaining sample volume (from the dialysis bag) was weighed, and 6 ul of the sample was taken and stored separately at 4°C. Then, the sample solution was reinjected into the bag. In the end, the 6-ul samples were diluted (1/1000) and measured by the ELISA assay. The percentage of SynO4 released was determined as follows:

Equation 1: $m_{SynO4(x\ hour)} = C_{SynO4}$ *[mg/ml, ELISA] x remaining sample volume in each time point [ml]*

Equation 2: $\%_{SynO4\ remaining\ in\ dialysis\ bag} = m_{SynO4(x\ hour)} / m_{SynO4(0\ hour)}\ x\ 100$

Equation 3: $\%_{SynO4\ released\ in\ the\ external\ buffer} = 100 - \%_{SynO4\ remaining\ in\ the\ dialysis\ bag}$

Stability characterization of BTL

The size and particle concentration of BTL samples stored at 4ºC and 25ºC were measured at six-day intervals over a total period of 31 days using a Zetasizer Ultra instrument. The activity percentage of the encapsulated SynO4 mAbs was assessed every seven days, resulting in a total of five measurements, using the developed ELISA assay.

Percentage of TF molecules on the surface of BTL

The nanoparticles' surface area occupied by TF molecules was quantified as follows:

Equation 1: $Units_{TF}$ *x* πr^2 *(surface area of a head cylinder) =* $95\pm23 \times \pi(2.4\,nm)^2 =$ $1716.9\pm422\ nm$

Equation 2: $4\pi r^2$ *(surface area of a sphere (liposome)) =* $4\pi(59.7\ nm)^2 = 44787.7\ nm$

Equation 3: *%TF molecules = UnitsTF x* πr^2 *(surface area of a head cylinder) /* $4\pi r^2$ *(surface area of a sphere (liposome)) x 100% = 3.8%±0.9%*

Conjugation of gold nanoparticles to transferrin-liposomes

GNPs were attached to transferrin-liposomes using a 5 nm NHS-Activated Gold Nanoparticle Conjugation Kit (Cytodiagnostics Inc, Canada, CGN5K-5-2). First, 10^13 particles/ml transferrin-liposomes or untargeted liposomes (negative control) were mixed with 5 nm NHS-GNPs [10^13 particles/ml] and then incubated at 25ºC for 2 hours. The reaction was then stopped by adding a quencher solution, according to the manufacturer's instructions. Next, the GNPs were bound covalently to transferrin-liposomes through the amine groups of the TF molecules. Finally, the GNP-transferrin-liposomes and GNP with the unconjugated untargeted liposomes samples were imaged with cryo-TEM. Semiquantitative data of the minimal distance [nm] between the GNPs and the lipid membrane was calculated using a code written in Fiji imaging software analysis[39] (**Figure S7**).

Cryo-TEM

Cryo-TEM imaging was performed using an FEI (Thermo Fisher Scientific) Talos 200C high-resolution TEM (Center for Electron Microscopy of Soft Matter, Wolfson Department of Chemical Engineering, Technion). The specimens were prepared at 25°C and 100% relative humidity within a controlled environment vitrification system. Drops of diluted liposomes were placed in a carbon-coated perforated polymer film, mounted on a 200-mesh TEM grid, and manipulated using tweezers. 10^10 particles/ml GNPs-transferrin-liposomes or GNP with unconjugated untargeted liposomes were used for the imaging measurement; in the case of the BBB *in-vitro* crossing evaluation, a 24-hour medium sample with transferrin-liposomes

was taken for imaging without a dilution step. After being thinned with a filter paper-covered metal strip, the drop was immersed in liquid ethane at its freezing point (-183°C). Then, under controlled conditions, the grid was transferred into a Gatan 626 (Gatan, Pleasanton, CA) cryo-holder and imaged at -175°C. Digital images were captured using a highly sensitive FEI Falcon III direct-imaging camera. A volta phase plate was used to enhance the contrast of the images.

Dye-labeled liposomes synthesis

Cy5-labeled liposomes, Cy3-labeled liposomes, or AZDye 647-labeled liposomes were prepared using the thin-film method, as described above. Shortly, 1,2-distearoyl-sn-glycero-3-phosphoethanolamine (DSPE) (Lipoid, Germany, 565400) was mixed with Cy5 se(mono so3) (Cy5; BLD pharm, China, BD759435), Cyanine3 NHS ester (Cy3; Abcam, UK, ab146452) or AZDye 647 NHS ester (CLICK CHEMISTRY TOOLS, USA, 1344-5) in a molar proportion 1:1 (DSPE: Dye) to yield Cy5-DSPE synthesized lipids, Cy3-DSPE synthesized lipids and AZDye 647-DSPE synthesized lipids. Then, the labeled lipid was added to the lipid mixture at a 0.4% molar ratio, meaning that the composition of the labeled liposome was DPPC: Chol: DSPE-PEG2000-NH2: DSPE-PEG1000: DSPE-Dye in molar percentages of 59.6:30:2.5:2.5:0.4.

To maintain a constant number of TF units per liposome surface, Dye-DSPE was added to all liposome preparations.

Dye-labeled SynO4 antibody synthesis

The dye-labeled SynO4 antibody was prepared using the EDC/NHS coupling reaction. Shortly, SynO4 antibody (2 mg/ml) was mixed with Cyanine3 NHS ester or Cy5 se(mono so3) at a molar proportion of 1:10 for 2 hours, at a pH of 8.4, at 25ºC. Then, the reaction solution was dialyzed against PBS pH 7.4 (1:1000 volume ratio) using a 12-14 kDa dialysis membrane; the external buffer was exchanged three times (after 1 hour, 4 hours, and overnight). Finally, the absorbance of the Cy3-labeled SynO4 antibody or Cy5-labeled SynO4 antibody was read at 280 nm by a plate reader. Finally, using the following equation, the number of dye molecules per antibody was calculated:

Equation 1: $Dye/mAb = A_{Dye} \times \varepsilon_{mAb} / (A_{mAb} - A_{Dye} \times CF) \times \varepsilon_{Dye}$

*$\boldsymbol{A_{Dye}}$ – optical density of the sample at dye absorption maximum; $\boldsymbol{A_{mAb}}$ – sample optical density at 280 nm; $\boldsymbol{\varepsilon_{mAb}}$ – molar extinction coefficient of antibody at 280 nm (210,000 for IgG); $\boldsymbol{\varepsilon_{Dye}}$ – molar extinction coefficient of dye at absorption maximum (162,000); **CF** – correction factor for dye (0.09 for Cy3 and 0.04 for Cy5).*

In all the dye-antibody conjugations, the ratio of dye/mAb was between 2 and 4.

Cell culture

Each cell line or primary culture was cultured at 37°C in a humidified atmosphere containing 5% CO_2, and a fresh medium was added every 2-3 days.

hCMEC/D3 immortalized human brain capillary endothelial cells (MERCK) were provided by A. Sosnik (Laboratory of Nanomaterials Science, Department of Materials Science and Engineering, Technion). Cells (adherent) were cultured in EndoGRO-MV Complete Media Kit (MERC, USA, SCME004) supplemented with 1 ng/ml FGF-2 (MERC, USA, GF003). Cell plating was performed on a flask coated with Collagen Type I, Rat Tail (MERC, USA, 08115) solution in PBS (MERC, USA, BSS-1005-B) at a dilution of 1:20 and then incubated for 1 hour, at 37°C. Then, trypsin-EDTA (MERC, USA, SM2003C) was used to dissociate the cells.

SH-SY5Y (ATCC) is a thrice-cloned subline of the neuroblastoma cell line SK-N-SH (cells were provided by A. Fishman, Laboratory of Molecular and Applied Biocatalysis, Faculty of Biotechnology and Food Engineering, Technion). Cells (adherent) were cultured in a complete media based on a 1:1 mixture of Dulbecco's Modified Eagle's Medium (DMEM, Sigma-Aldrich, Israel, D5796) and Nutrient Mixture F12 HAM with Sodium B (Sigma-Aldrich, Israel, N4888) with supplemented with 1% (v/v) Penicillin (10,000 units/ml), Streptomycin (10 mg/ml) (Pen-Strep, Biological Industries, Israel, 030311B), 1% (v/v) Amphotericin B (2.5 mg/ml) (Amp-B, Biological Industries, Israel, 030281B), 10% (v/v) FBS, and 1% (v/v) non-essential amino acids (Biological Industries, Israel, 013401B). In general, the cells were dissociated and harvested using a cell scraper.

For the neuronal differentiation, SH-SY5Y cells were seeded on 1% Gelatin from Porcine Skin, Gel Strength 300, Type a (Sigma-Aldrich, Israel, G2500) coated plates and then incubated with the complete media supplemented with 10uM All-Trans Retinoic Acid (RA, Sigma-Aldrich, Israel, R2625) for 4 days. Then, the medium was replaced with a starvation media (complete media without FBS) supplemented with 50 ng/ml Human BDNF factor (PeproTech, Israel, 4500210) for an additional 4 days; the cells were fully differentiated after 7 days.

Cortical neuronal cultures of P1 and P2 mice pups (ICR strain) were established and provided by U. Ashery lab (School of Neurobiology, Biochemistry, and Biophysics, George S. Wise Faculty of Life Sciences, Sagol School of Neuroscience, Tel Aviv University) and were produced as previously described.[40] Cells were plated into a 6-well plate (500,000 cells/ml) on a glass coated with a MatriGel (Corning, USA, 354230) solution in Hanks Balanced Salt Solution (HBSS, Sigma-Aldrich, Israel, H1387) and 20 mm HEPES buffer (Biological Industries,

Israel, 030251B). Neurons were grown in Neurobasal A (NBA, Gibco, Ireland, 10888022) supplemented with B-27 (Gibco, Ireland, 17504044), GlutMax (Gibco, Ireland, 35050061), Pen-Strep, and 5% fetal calf serum (FCS, Gibco, Ireland, 10270106) to support glia growth on the day of culture preparation. From the following day, the medium was exchanged twice a week with a growth medium, which contained no serum and was similar to the plating medium, to avoid the proliferation of glial cells.

Dopaminergic neurons were derived from human PD patient's iPSCs with 4 copies of an SNCA gene mutation (AS gene), as previously described[32], and cultured in the S. Stern lab (Sagol Department of Neurobiology, Faculty of Natural Sciences, University of Haifa). Briefly, human iPSCs of a PD patient were grown in mTesRTM plus medium (Stem Cell Technologies, Canada, 05825) until the culture was ~80% confluent. The iPSC colonies were then dissociated into a single-cell suspension using an accutaseTM (Thermo Fisher Scientific, USA, A1110501) treatment for 5 minutes, followed by the addition of trypsin inhibitor (Sartorius, Germany, 03-048-1C) to stop the dissociation. The dissociated cells were then re-plated on Matrigel (R and D systems, USA, 3433-010)-coated plates in mTesRTM plus media at a density of 40,000 cells/cm^2. After two days of daily media changes, the cells reached ~50% confluency. At this point (Day 0), the differentiation process was started using KSR media-DMEM F-12 (Thermo Fisher Scientific, USA, 11320033), with Glutamax 1X (Thermo Fisher Scientific, USA, 35050061), 15% KO-SR (Thermo Fisher Scientific, USA, 10828028), 1% NEAA (Thermo Fisher Scientific, USA, 11140050), 1% Antibiotic-Antimycotic (Thermo Fisher Scientific, USA, 15240096), and 0.1 mM β-mercaptoethanol (Sigma-Aldrich, Israel, M6250). The medium was then changed gradually to N2 medium-DMEM F-12 with Glutamax 1X, 1% N2 supplement (Thermo Fisher Scientific, USA, 17502048), 1% Antibiotic-Antimycotic (for Days 5 and 6: 75% KSR: 25% N2; for Days 7 and 8: 50% KSR: 50% N2; for Days 9 and 10: 25% KSR: 75% N2). Finally, the medium was changed to B27 medium on Day 11 (Neurobasal medium (Thermo Fisher Scientific, USA, 21103049), 2% B27 supplement (Thermo Fisher Scientific, USA, 17504044), 1% Glutamax, 1% Antibiotic-Antimycotic, 10 ng/mL BDNF, 10 ng/mL GDNF (PeproTech, Israel, 45010), 1 ng/mL TGFβ3 (PeproTech, Israel, 100-36E), 0.2 mM Ascorbic acid (Stem cell technologies, Canada, 72132), and 0.1 mM cAMP (TOCRIS, UK, 1141). During the differentiation process, the following small molecules were also added to the culture medium: 10 M SB431542 (Cayman Chemical, USA, 13031) on Days 0-4; 100 nM LDN-193189 (BioGems, USA, 1066208) on Days 0-12; 2 M Purmorphamine (Cayman Chemical, USA, 10009634), 0.25 M SAG (Cayman Chemical, USA, 11914) and 100 ng/mL FGF8b (PeproTech, Israel, 100-25) on Days 1-6; 3 M CHIR99021 (Cayman Chemical, USA, 13122) on Days 3-12. Half of the media was changed every other day. After 20 to 25 days of differentiation, the neurons were dissociated for the second time using accutaseTM and trypsin inhibitor (as described above), re-plated onto Matrigel-coated 48-well coverslips and allowed to differentiate in B27 medium until day 30. From day 30 onward, the basal medium was

gradually replaced with BrainphysTM (Stem cell technologies, Canada, 05790) medium (instead of DMEM-F12), which helps in forming synaptic connections.

Evaluation of PEG tail length on liposomes' **cellular uptake in hCMEC/D3 and TF** targeting capacity

hCMEC/D3 cells were seeded (75,000 cells/ml) 1 day before the experiment. On the day of the experiment, PEG2000-TF/PEG1000 and PEG2000/PEG1000 Cy5-labeled liposomal formulations were prepared as previously described. Additional, PEG2000-TF/PEG2000 and PEG2000 Cy5-labeled liposomal formulations were prepared in molar percentages of 59.6(DPPC): 30(cholesterol): 2.5(PEG2000-TF): 2.5(PEG2000): 0.4(Cy5-DSPE) and 59.6(DPPC): 30(cholesterol): 5(PEG2000): 0.4(Cy5-DSPE), respectively. The hCMEC/D3 cells were incubated for 30 min with the different Cy5-labeled liposomal formulations to a final concentration of 0.5mM total lipids, corresponding to ~ 10^12 liposomes/ml. Then, the culture medium was removed, and the cells were rinsed with PBS three times, incubated with Trypsin-EDTA for 4 min in heating, and centrifuged at 500g for 7 min. Finally, the cell pellet was resuspended in fresh medium supplemented with 5% (v/v) FBS. Cellular uptake was detected in the Cy5 channel after acquiring 30,000 cells per sample using a flow cytometer (FACS; BD LSR-II, BD biosciences, USA). Analyses were performed using FCS Express (De Novo software).

The effect of the amount of TF conjugated to the surface of the liposomes on cellular uptake in hCMEC/D3 was evaluated similarly. Five different formulations of Cy5-labeled BTL (empty) were prepared with TF concentrations ranging from 1-20 mg/ml. The conjugation of TF protein to liposomes was described previously; in this case, the amount of TF mixed with the liposomes varied in each formulation; labeled untargeted liposomes were used as a negative control (**Figure S8**).

Super-resolution imaging of BTL cellular uptake in endothelial cells

hCMEC/D3 cells were seeded (45,000 cells/ml) one day before the experiment. The next day, they were incubated overnight with Cy5-labeled BTL (empty) to a final concentration of 2.5mM total lipids, corresponding to 2.20×10^{13} liposomes/ml. Then, the culture medium was removed, and the cells were rinsed with PBS 3 times and fixed with cold 4% Paraformaldehyde (PFA) for 10 min. The cells were then permeabilized (0.1% Triton X100 for 5 min), blocked (10% FBS in 0.05% Tween20 in PBS for 30 min), and stained with Anti-Transferrin Receptor Antibody (Abcam, UK, ab84036) at 5 ug/ml in blocking serum for 1 hour. Next, they were stained with Goat Anti-Rabbit IgG H&L conjugated Alexa Fluor 488 (Abcam, UK, ab150077) at a dilution of 1:1000 in blocking serum for 1 hour and then rinsed with PBS (3 times) (**Figure**

S9). Acquisition and processing were performed using super-resolution (SR) microscopy (Elyra 7 eLS, Zeiss, Germany) and ZEN software and applying the 405-, 488-, 561-, and 642- nm lasers.

In-vitro BBB model of the neurovascular unit (NVU)

BMECs were differentiated from iPSCs (BGU003 passage 16-18), prepared as described in Neal et al. and Vatine et al.[41] with the following modifications: 24 hours before differentiation, iPSCs were seeded on Matrigel-coated plates (Corning, USA, 354234) at 20,800 cells/ml. The differentiation was started by culturing the cells in DMEM/F12 medium supplemented with 20% Knockout serum (Gibco, Ireland, 10828010), 1% non-essential-A amino-acids, 1 mM L-glutamine (Gibco, Ireland, 25030149), 216µM β mercaptoethanol (Gibco, Ireland, 31350010), 100 U/ml Penicillin, and 100 ug/ml Streptomycin (Biological Industries, Israel, 030311B). The medium was changed daily for 4 days. Then, the medium was switched to endothelial serum-free medium (Gibco, Ireland, 11111044) supplemented with 20 ng/ml bFGF (Peprotech, Israel, 10018B), 10 µM retinoic acid, B-27 (Gibco, Ireland, 12587010), 100 U/ml Penicillin, and 100 ug/ml Streptomycin, for 2 days, and then re-seeded on 3 µm pore Transwells (Greiner, Osterreich) coated with 400 ug/ml human collagen type IV (Sigma-Aldrich, Israel, C5533) and 100 ug/ml human fibronectin (Corning, USA, 356008), at least 4 hours before seeding. Cells were seeded at $2x10^5$ cells per 24-well Transwell. The medium was replaced the day after with endothelial serum-free medium supplemented with B-27, 100 U/ml Penicillin, and 100 ug/ml Streptomycin, and was changed every other day. The barrier function and density of the cell layers were evaluated by TEER measurements (Millicell ERS-2 Voltohmmeter, Merck Millipore) daily; after ten days of differentiation, a TEER value of 154±9 ohm*cm^2 was obtained, and it was determined as an optimal value for the experiment.

For the liposome transport experiments, iPSC-derived BMECs cultured in Transwells were placed on top of a primary cortical neuron culture transduced with a pAAV-hSyn1-EGFP-(P2A)-α-Syn A53T-HA tag viral vector. For control, Transwells without a layer of BMECs were used; liposome transport was faster on Transwells without a layer of BMECs.

For the live imaging experiments, 5 mM Cy5-labeled BTL (empty) were added to the donor chamber at different times (1, 4, 27, and 36 hours). Then, the BMECs were fixed for immunostaining of ZO-1 (cell signaling), and image acquisition was done with a confocal microscope (Olympus IX=83) to allocate labeled liposomes at the Z position.

Permeability of BTL across the *in-vitro* BBB model

To determine the permeability of BTL (empty) across the BBB, the particles were prepared and added to the donor chamber at a concentration of 5mM total lipids, corresponding to $1.05x10^{13}$ liposomes/ml. Medium samples (50 ul) were extracted from the acceptor chamber at 1, 2, 4, and 24 hours and read by a plate reader at λ_{ex}=633 nm and λ_{em}=685 nm; there was a chamber for each time point, so a fresh medium was not required to replace the medium taken. The cells were kept under culture conditions during the transportation experiment. The liposome concentration was calculated using a calibration curve of Cy5-labeled BTL (empty); concentration versus intensity.

Live imaging of BTL transport through the BMEC layer

A "Well-Chip" (**Movie S2**) was developed to image the BTL transport, ensuring high-quality imaging and higher throughput. The “Well-Chip” was based on the concept of our previously reported chips, which is to create a modular system for imaging.[42] It was created via a Polydimethylsiloxane (PDMS) sheet prepared by Sylgard 184 (Sigma-Aldrich, Israel, 761028) mixed with 1:10 curing agent, followed by curing at 60℃for at least 4 hours. PDMS sheets were cut to fit a 12x60mm cover glass and punched with 3 holes (ID 10mm) to fit a Transwell assembly, as shown in the description of Movie S2. The cut PDMS sheets were cleaned in EtOH, dried at room temperature, activated in oxygen plasma (Atto-BR-200-PCCE, Diener Electronic, Germany) for 30 sec, and assembled on the cover glass. Inside each "Well-Chip" was inserted a ring (outer diameter 9.5mm, inner diameter 7.5mm) to hold the Transwell at a specific height, designed in SolidWorks CAD software (SolideWorks Corporation, USA), and printed in a Form3 3D printer (Formlabs, Somerville, USA) using clear resin. Custom “Well-chips” were sterilized by EtOH washes and UV light for 30 minutes.

Following the preparation of the platform, the Transwells were added to the "Well-Chip", and the Cy5-labeled BTL were added to the upper side of the Transwell where BMECs were seeded. BTL transport was followed by an Olymus IX-83 confocal microscope over 20 hours in Z-stack. Time-lapse image analysis of the BTL at different membrane levels was conducted using the ImageJ software.[39] The lowest level is z=1 below the cells, the highest level is z=70 above the cells, and the membrane level is z=40 (**Figure S11c**).

Evaluation of BTLs’ endolysosomal pathway in brain sections

Three 7–8-week-old female C57/6JOlaHsd mice (Envigo, Israel) were deeply anesthetized (8.5 mg/ml ketamine, 1.5 mg/ml xylazine, in 100 ul saline) and injected retro-orbitally with 50 ul of AZDye 647-labeled BTL (empty) (50 mM; 1.79E+13 particles/ml). The particles were allowed to circulate for 30 minutes or 6 hours. Brains were dissected, fixed in 4% PFA at 4°C overnight, cryopreserved in 30% sucrose, and frozen in TissueTek OCT (Sakura, Japan).

Frozen brains were cut into 6 um slices for dSTORM imaging (CM1950, Leica, Germany) to produce coronal brain sections. Then, the slices were mounted on poly-D-lysine coated coverslips (Marienfeld-Superior, Germany, no. 1.5H). dSTORM imaging was performed in a freshly prepared imaging buffer containing 50 mM Tris (pH 8.0), 10 mM NaCl, and 10% (w/v) glucose with an oxygen-scavenging GLOX solution (0.5 mg/ml glucose oxidase; Sigma-Aldrich, Israel, G2133), 40 ug/ml catalase (Sigma-Aldrich, Israel, C40), 10 mM cysteamine MEA (Sigma-Aldrich, Israel, 30070), and 1% ß mercaptoethanol.[43] A Nikon Ti-E inverted microscope was used. The Nikon STORM system (N-STORM) was built on TIRF illumination using a 1.49 NA X100 oil immersion objective and an ANDOR DU-897 camera. The primary antibodies, Rabbit GLUT1 Polyclonal antibody (Millipore, USA, #07-1401) at a 1/400 dilution and Rat LAMP1 Monoclonal antibody (DSHB, USA, 1D4B) at a 1/100 dilution, were applied to the tissue sections and incubated. For secondary antibody staining, an Anti-Rat IgG Alexa fluor-488 (Jackson, USA, 712-545-153) and an Anti-Rabbit IgG CF568 (Biotium, USA,20098) were used at dilutions of 1/400 and 1/800, respectively. 488, 568, and 647 laser lines were used for activation with a cycle repeat of ~4000 cycles for each channel. Nikon NIS Element software and ThunderSTORM (NIH ImageJ)[44] software were used for acquisition and analysis. We used the dSTORM approach which is based on labeling the target protein with a primary antibody and then using a secondary antibody conjugated to a fluorophore. Thus, resolved signals represent a location that is approximately 40 nm from the actual epitope (assuming the approximation of the two antibodies' length in a linear conformation). A resolution of approximately 20 nm allowed us to separate signals and use these as proxies for the abundance of target molecules, which can reliably be used to compare different states. Single-molecule localization microscopy (SMLM) results in point patterns with specific coordinates of individual detected molecules. These coordinates are typically summarized in a 'molecular list' (provided by ThunderSTORM analysis.[44] Colocalization analysis to determine the proximity of BTL to the LAMP1 marker (lysosomes) was performed using NIH ImageJ. In order not to underestimate lysosomal localization, colocalization was defined as a distance less than 100nm between liposomes and lysosome markers. A total of 15 capillaries were analyzed from 3 mice.

All the mice in the experiment were maintained in the animal facility of the Hebrew University under specific pathogen-free conditions. All animals were treated according to institutional guidelines approved by the Institutional Animal Care and Use Committee (IACUC) at Hebrew University (protocol MD-21-16361-5).

Studying the spatial and temporal dynamics of BTLs' penetration into neuronal brain cells

In utero electroporation was performed on E14.5 timed pregnant ICR dames. The lateral ventricle of embryos was injected with a plasmid encoding CAG-mEGFP at a concentration of 1 ug/µl with 0.01% Fast Green dye. Five electrical pulses (45V, 50-ms duration, 1 Hz) were delivered using a NEPA21 electroporator (NEPAGENE). Following birth, GFP-positive pups were identified and left to mature until p30. For cranial window surgery, mice were

anesthetized with isoflurane, placed in a stereotaxic frame, and the skin and skull were exposed. A dental drill was used to perform a 2.5-3 mm circular craniotomy centered over the GFP-positive region. The skull was sealed using a cover glass, which was secured and attached to the exposed skull along with a head plate to secure the head during imaging using dental cement. Mice were left to recover on a heating pad, and were used for 2pFLIM imaging before, and then after, the intravenous injection of 350 ul 50 mM of Cy3-labeled BTL ($1.68x10^{13}$ particles/ml) through the tail vein. For *in-vivo,* 2pFLIM, GFP, and Cy3 were excited with a Ti: sapphire laser (Chameleon, Coherent) at a wavelength of 920 nm and a power of 10-30 mW. Fluorescence lifetime images were obtained using a Bergamo two-photon microscope (Thorlabs) equipped with a Time-Correlated Single Photon Counting board (Time Harp 260, Picoquant). Emission was collected with a 16×0.8 NA objective (Nikon), divided with a 565-nm dichroic mirror (Chroma), and detected with two Photo-Multiplier Tubes with low transfer time spread (H7422-40p, Hamamatsu). Images were collected by 128×128 or 256x256 pixels, acquired at 2 ms/line, and averaged over 24 frames. The fluorescence lifetime of GFP and Cy3 was measured by curve fitting using custom software written with C#, as described previously.[26] For analysis, TauD and TauAD values for GFP and Cy3 were fixed at 2.6 and 1.0 ns respectively. A double exponential fit was calculated for ROI placed on cell bodies and neurites. The difference in lifetime was calculated between a corresponding Cy3-labeled BTL-positive puncta and a nearby GFP background region (**Figure S12**). All animal experiments were approved by the Tel Aviv University Committee on Animal Care.

Construction of a pAAV-hSyn1-eGFP-P2A-alpha-synuclein A53T-HA tag target plasmid

To construct an adeno-associated virus (AAV) vector that exploits the human synapsin-1 promoter to drive the expression of eGFP and Alanine 53 to a Threonine mutant alpha-synuclein linked by a self-cleaving P2A peptide, an A53T mutation by Inverse PCR applying primers hSynuclein A53T.FOR (5'–ACAACAGTGGCTGAGAAGACC- 3') and hSynuclein A53T.REV (5'–CACACCATGCACCACTCCC – 3') and a lentiviral plasmid pCMV-eGFP-wild type alpha-synuclein-HA tag as a template. Next, the HA-tagged A53T mutant alpha-synuclein gene was subcloned by Gibson assembly into NcoI and HindIII sites of plasmid pAAV-hSyn1-eGFP-P2A-eGFPf-WPRE-HGHpA (Addgene, USA, 74513), applying lentiviral plasmid pCMV-eGFP-α-Syn-Puro A53T mut-HA tag as a template and the forward and reverse primers Syn-NcoI-gib.FOR (5' – TGAAACAAGCAGGGGATGTCGAAGAGAATCCCGGGCCAGCCATGGATGTATTCATGAAAGGACTTT CAAAGG – 3') and Syn-HindIII-gib.REV (5' – TCTTTCACAAATTTTGTAATCCAGAGGTTGATTATCGATAAGCTTTTAAGCGTAATCTGGAACATCGT ATGGG – 3'). The DNA sequencing analysis was used for the plasmid integrity validation (**Figure S13**).

AAV production and infection of primary neurons

To express the eGFP-P2A-aplpha-synA53T-HA fusion protein in mouse primary cortical neurons, an AAV delivery system was used. ProAAV HEK-293T cells were transfected with the helper plasmids PHP.eB, pADdeltaF6, PHP.S (Addgene, USA, 103005, 112867, and 103006) and with a target plasmid pAAV-hSyn1-eGFP-P2A-α-synA53T-HA tag bearing the eGFP-P2A-α-synA53T-HA fusion protein under control of the human synapsin promoter. Briefly, ProAAV HEK-293T packaging cells growing in 15-cm dishes were transfected with a mix of 20 µg helper vector PHP.eB / PHP.S, 20 µg helper vector pADdeltaF6, and 20 µg target plasmid: pAAV-hSyn1-eGFP-P2A-α-synA53T-HA. JetPI transfection reagent (Polyplus, Paris, 101-10N) was used as a transfection reagent under poor nutrients media: 1% glutamax, high glucose DMEM. 18 hours post-transfection, the culture media was replaced with a fresh rich-serum medium containing 2% P/S, 20% FBS, 1% glutamax, and high glucose DMEM. After 48 hours of incubation, ProAAV HEK cells were detached by 0.5 M EDTA, and the AAV particles were extracted, purified, and concentrated according to the AAVpro® Purification Kit Maxi (TaKaRa, Japan, 6666). Quantitative PCR for AAV titer measurement was performed by applying SYBR green fastmix (Quantabio, USA, 95073-250), forward ITR primer 5'-GGAACCCCTAGTGATGGAGTT, and reverse ITR primer 5'-CGGCCTCAGTGAGCGA. Readouts were compared to a calibration curve of a known concentration of an AAV backbone plasmid. Primary mouse cortical neurons were infected with α-synA53T AAV particles overnight. The culture medium was replaced by a fresh medium and neurons were further incubated for 7 days without changing the medium (**Figure S13**).

Confocal imaging of BTL cellular uptake in PD primary neurons

Confocal microscopy (LSM 710, Zeiss, Germany) was used to examine the liposomal uptake and antibody payload release in PD primary neurons (**Figure 3B**). Overexpressed AS PD primary neurons were prepared using AAV developed with HEK293T (ATCC) cells, using high-titer AAV2 virions pseudotyped with RepCap-DJ packing, pAdenohelper, and a pAAV-hSyn1-EGFP-(P2A)-α-Syn A53T-HA tag (**Figure S13**). The cells were seeded (500,000 cells/ml), and on day 3, transduced with the engineered AAV virus in their growth media; the entire medium was replaced on day 4. On day 8, the cells were treated either with free Cy3-labeled SynO4 antibody (3.95 ug/ml) or with 2.5mM Cy5-labeled BTL loaded with Cy3-labeled SynO4 overnight. The following day, the medium was removed, and the cells were washed (3 times with PBS), fixed (4% PFA for 10 min), permeabilized (0.25% Triton X100), blocked (5% Normal Goat Serum (Vector Laboratories Inc, USA, S-1000) with 1% Bovine Serum Albumin (BSA, VWR Chemicals, USA, 0332-TAM)), and immunostained with Rabbit Monoclonal Anti-Alpha-Synuclein (Abcam, UK, ab212184) and Goat Anti-Rabbit CF568 (1:500; Biotium, USA, 20801); the cells were stained with Hoechst (1 ug/ml) for nuclei labeling. The entire procedure was carried out in the U. Ashery Lab. The imaging was performed in the LSE infrastructure center (Technion). The acquisition was conducted using the ZEN software and 405-, 488-, 543-, and 639- nm lasers.

FACS quantification of BTL uptake *in vitro*

SH-SY5Y cells were seeded (120,000 cells/ml) 7 days before the experiment and treated with RA and BDNF reagents to ensure full differentiation. Wells were transduced for 24 hours with AAV1/2-CMV/CBA-human-A53T-alpha-synuclein-WPRE-BGH-polyA vector in a titer of $5x10^{11}$ GC/ml (PD-induced cells). On day 2, the PD cell medium was removed, and some wells were treated overnight with Cy3-labeled SynO4 mAbs (4.06 ug/ml) or Cy5-labeled BTL loaded with Cy3-labeled SynO4 mAbs (2.5 mM); fresh medium was added to the untreated wells. On day 3, the medium from all the wells was removed, and the cells' wells were washed 3 times with PBS and then dissociated with Cell Dissociation Buffer mixed with 10% FBS solution. The buffer was centrifugated at 500g for 7 min. Next, the cells' pellets were resuspended in a 5% FBS solution. The cells were then analyzed with a spectral flow cytometer (Cytek Aurora, CYTEK, USA), with 100,000 events counted per sample. The results were analyzed using FCS Express software. The results (1 independent repetition performed in 5 replicates) are presented as mean±SD. Two-tailed unpaired Student's t-test was used for the statistical analysis; ***p<0.0001.

Super-resolution *im*aging of BTL cellular uptake in differentiated PD-SH-SY5Y cells

Cells were seeded (75,000 cells/ml) 7 days before the experiment and treated with RA and BDNF reagents for full differentiation. Next, the cells were incubated with 2.8 ug/ml Recombinant Human Alpha-Synuclein Protein aggregates Active (Abcam, UK, ab218819) labeled with an Alexa Flour 488 Conjugation Kit (Abcam, UK, ab236553) for 6 hours to establish PD neurons. The culture medium was then removed, and the cells were rinsed with PBS 3 times and incubated overnight with Cy5-labeled BTL loaded with Cy3-labeled SynO4 (2.5Mm), free Cy3-labeled SynO4 (3.65 ug/ml), or Cy5-labeled BTL (empty) (2.5mM, control). The next day, the medium was removed, and the cells were rinsed with PBS (3 times) (**Figure S14a and b**) and stained with Hoechst staining (1 ug/ml; Sigma-Aldrich, Israel, 63493) for nuclei labeling in both experiments. Acquisition and processing were performed using super-resolution (SR) microscopy (Elyra 7 eLS, Zeiss, Germany) and ZEN software and by applying 405-, 488-, 561-, and 642-nm lasers.

Quantitative imaging analysis of *in-vitro* studies

The confocal images of PD primary neurons were analyzed by the IMARIS software. An analysis was conducted to measure the amount of SynO4 antibody inside each neuron, normalized by the number of neurons per field (at least 9 fields of 3 independent repetitions). Furthermore, super-resolution images (**Figure S14c and d**) of PD-SH-SY5Y were analyzed by

the IMARIS software, allowing the semiautomated tracing of SynO4 antibody colocalization with AS aggregates, as well as the percentage of SynO4 antibody released from BTL. These parameters and statistics were measured for at least 18 fields of 3 independent repetitions.

Confocal imaging of BTL cellular uptake in PD-SH-SY5Y cells

The cells were seeded (120,000 cells/ml) 7 days before the experiment and treated with RA and BDNF reagents for full differentiation. Next, some of the cells' wells were incubated with 0.2 uM Recombinant Human Alpha-Synuclein Protein aggregates Active labeled with an Alexa Flour 488 Conjugation Kit for 6 hours to establish PD neurons, while the remaining wells were left untreated (representing a healthy control group). The culture medium was then removed, and the cells were rinsed with PBS 3 times and incubated overnight with Cy3-labeled BTL loaded with Cy5-labeled SynO4 (2.5Mm), free Cy5-labeled SynO4 (4.25 ug/ml), or Cy5-labeled BTL (empty) (2.5mM, control). The next day, the medium was removed, and the cells were rinsed with PBS (3 times) and stained with Hoechst staining (1 ug/ml; Sigma-Aldrich, Israel, 63493) for nuclei labeling in both experiments. The imaging was performed in the LSE infrastructure center (Technion). The acquisition was conducted using ZEN software and by applying 405-, 488-, 543-, and 639-nm lasers (**Figure S15**).

*d*STORM microscopy

Healthy primary and PD primary neurons transduced with the engineered AAV virus (day 3) were seeded (500,000 cells/ml). On day 8, the cells were incubated overnight with a free SynO4 antibody (3.95 ug/ml) and BTL (2.5mM). The following day, the medium was removed, the cells were washed (3 times with PBS), fixed (4% PFA for 10 min), permeabilized (0.25% Triton X100), blocked (5% Normal Goat Serum with 1% BSA), and immunostained with Rabbit Monoclonal Anti-Alpha-Synuclein and Goat Anti-Rabbit CF568.

Super-resolution acquisition

Direct Stochastic Optical Reconstruction Microscopy (dSTORM), super-resolution imaging was done using a single-molecule localization microscope (Vutara 350, Bruker). The manufacturer Vutara 350's defined precision is 20 nm XY and 50 nm Z resolution. The actual microscope's lateral resolution ranges between 15nm - 40nm and its axial resolution ranges between 50nm - 80nm. It's important to state that we were not using Z-stack imaging since we were imaging the sample at one Z plane. The Vutara350's custom case is designed for super-resolution, environmental isolation, temperature regulation, and drift minimization.

Bruker patented Biplane technology offers higher localization precision than astigmatism over a larger axial range, making it the preferred commercial 3D super-resolution technique. In

comparison to astigmatism, the Biplane technique offers an enhanced per-pixel SNR resulting in superior localization precision. The Biplane and Quadfield modules detect the PSF from two different focal planes and sum the total number of photons, which yields superior localization precision over a larger axial range (without the perceived loss of photons). The cameras used are a sCMOS camera (4 MP, 6.5 m x 6.5 m pixel size for super-resolution imaging) and a CCD camera (1392x1040 for widefield imaging). All imaging was done using water immersion 60x objective NA 0.13-0.21 / FN26.5. and 1000mW lasers. To enable single-molecule photoswitching of the dyes Alexa Fluor 647 and CF®568, the chamber was filled with imaging buffer B (50 mM Tris-HCl pH 8, 10 mM NaCl, 10 % (w/v) glucose) supplemented with 20 mM cysteamine (MEA; dissolved in buffer A (50 mM Tris-HCl pH 8, 10 mM NaCl)), 2 % (v/v) Gloxy (glucose oxidase (168.8 AU) and catalase (1404 AU) mixture in buffer A) and 1% (v/v) 2-mercaptoethanol. Image processing was carried out using the open-source software ImageJ[45] and home-written analysis software as detailed below.

Cluster analysis

For each condition, 10 dSTORM images of 4 independent replicates were randomly taken. A density-based clustering algorithm, Hierarchical Density-Based Spatial Clustering of Applications with Noise (HDBSCAN), was used to analyze the localizations extracted from each image. We used a built-in from the hdbscan-clustering library in Python. HDBSCAN determines the core distances for each localization to estimate its probability density function (PDF). The core distance of a point is its distance from its kth nearest neighbor; the denser the area, the smaller the core distance of a point is. The parameters we used were: minPoints = 50, and the extracting algorithm was 'leaf'. We applied noise reduction with Principal Component Analysis (PCA) with a standard deviation of 1.0. The PDF of a point is defined as the probability of being within a small region around it and can also be interpreted as the expected density around that point. Based on the mutual reachability distance, HDBSCAN assigns points to the clusters. The mutual reachability distance of a pair of points is the maximum value between the core distance of point 'a', the core distance of point 'b', and the distance between points 'a' and 'b'. Localizations of Connexin43 proteins in the dSTORM images were extracted as xy-coordinates and analyzed for cluster size, density, and number of localizations per cluster.

FACS evaluation of cell death

SH-SY5Y cells were seeded (120,000 cells/ml) 7 days before the experiment and treated with RA and BDNF reagents to ensure full differentiation. Wells were transduced 24 hours with either AAV1/2-CMV/CBA-human-A53T-alpha-synuclein-WPRE-BGH-polyA (Charles River,

USA, GD1001RV) vector in a titer of $5x10^{11}$ GC/ml (PD-induced cells) or hydrogen peroxide (H_2O_2; 0.2M, positive control), or not treated (healthy, negative control). On day 2, the PD cell medium was removed, and some wells were treated overnight with free SynO4 mAbs (0.042 ug/ml), Cy5-labeled BTL (empty) (0.05 mM) or Cy5- labeled-BTL (0.05 mM); to the remaining wells, fresh medium was added. On day 3, the medium from all the wells was collected, and the cells were dissociated with the Cell Dissociation Buffer (Rhenium, Israel, 13151014). The buffer was re-united with the medium and centrifugated at 500g for 7 min. Then, the cells' pellets were washed 2 times with PBS and resuspended in a binding buffer. Afterward, 5 ul Annexin V-FITC was added to the cell suspensions for 15 min in the dark, with 2.5 ul PI also added in the last five min. The cells were then analyzed with a spectral flow cytometer (Cytek Aurora, CYTEK, USA), with 30,000 events counted per sample. The results were analyzed using FCS Express software. Annexin V-FITC and PI double-positive cells were necrotic or late apoptotic cells. The experiments were performed using a MEBCYTO Apoptosis Kit (Annexin V-FITC Kit) (Enco, Israel, 4700).

AAV-based PD mice model establishment

Healthy 6-8-weeks-old c57BC/6JRccHsd male mice (Envigo, Israel) were anesthetized with 0.5% isoflurane and 1% O_2. Mice received a unilateral stereotactic injection of rAAV vector encoding alpha-synuclein - AAV2/6-hSyn1-Human SNCA-WPRE-polyA (Sirion Biolabs, Germany, SBSAA30004). Mice were next injected with 1.5 µl rAAV ($1.63x10^{13}$ GC/ml) directly to the right-side substantia nigra using an automated stereotactic injection device equipped with the mouse brain atlas; the machine was provided by the A. Zeisel lab, Technion. The injected animals' well-being was monitored for over 8 weeks. After 2, 4, and 8 weeks of viral injection, mice were sacrificed and an immunohistochemical and western blot analysis was conducted (**Figure S17**). It is important to note that all animal experiments were approved by the Inspection Committee on the Constitution of the Animal Experimentation at the Technion (IL0010120 and IL0330222) and that they were conducted according to its regulations.

Western blot analysis

Frozen brain sections of mice 2 weeks post PD induction were divided into right and left hemisphere samples and homogenized in lysis buffer. The initial homogenization was performed using a gentle MACS Dissociator (Miltenyi, Germany), followed by sonication on ice. Next, samples were centrifuged at 15,000xg for 1 hour at 4°C. The supernatant was termed "triton-soluble" and the pellet was re-suspended in lysis buffer with 2% Sodium dodecyl sulfate (SDS) and termed "triton-insoluble". Afterward, the protein concentration was determined using a Bradford Protein Assay Kit (BIO-RAD, Israel, 5000201). Then, 200 µg of protein extract was used to run an SDS-PAGE protein gel. Finally, a western blot was performed using

an Anti-Alpha-Synuclein antibody [MJFR1] (Abcam, UK, ab138501) and goat Anti-rabbit IgG-H&L (Abcam, UK, ab6721). It is important to note that the anti-human alpha-synuclein antibody does not react with mouse alpha-synuclein. Therefore, the western blot results refer solely to the human alpha-synuclein originating from the viral expression (**Figure S17d**).

RT-PCR analysis

6–8-week-old mice, 8 weeks post PD induction (via injection with 1.5 µl rAAV ($1.63x10^{13}$ GC/ml) directly to the right-side substantia nigra), PBS injection or no injection were sacrificed and perfused with ice-cold PBS. The brains were frozen using liquid nitrogen and kept at -80°C for further use. The brain's outer sections of the BBB area were peeled off using a scalpel and frozen in liquid nitrogen. The sections were ground to a powder in liquid nitrogen using a mortar and pestle. Total RNA was extracted using a NucleoSpin RNA Plus kit (Ornat, Israel, MAN740955), in accordance with the manufacturer's instructions. The extracted RNA's purity and quantity were evaluated using a plate reader, while its integrity was assessed using gel electrophoresis (2% agarose, 35 minutes at 100V). Next, 400 ng of RNA was converted to cDNA using a qScript cDNA Synthesis kit (Agentek, Quanta BioSciences, Israel, 95047500), following the manufacturer's protocol. Lastly, quantitative real-time PCR (qRT–PCR) was performed using qPCRBIO SyGreen Blue Mix Lo-ROX (Tamar LTD., Israel, PB201551) with cycling conditions implemented according to the manufacturer's instructions.

The qRT-PCR was measured in a QuantStudio1 (Applied Biosystems) real-time PCR thermal cycler. Then, the relative TF receptor expression was calculated using the $2^{-\Delta\Delta Ct}$ method. Before operating the qRT–PCR, specific primers (TF forward: AAACACAGACGTGCTCCATCA reverse: TCCTGCGTCCACTTTTGTCAT, and GAPDH forward: TGGGTGTGAACCACGAGAAA reverse: GGGCCATCCACAGTCTTCTG) were tested for their specificity (by analyzing dissociation curves ranging from 60-95°C), optimal concentration, and amplification efficiencies using standard no template and no enzyme controls.

In-vivo biodistribution

6–8-week-old mice, 8 weeks post PD induction (via injection with 1.5 µl rAAV ($8.15x10^{12}$ GC/ml) directly to the right-side substantia nigra), PBS injection or no injection were sacrificed and perfused with ice-cold PBS and healthy mice were intravenously injected (350 ul) either with Cy5-labeled untargeted liposomes or with Cy5-labeled BTL (empty); non-injected mice were used as a negative control. Twelve hours after injection, mice were euthanized and perfused with PBS, and their brains, lungs, livers, kidneys, hearts, and spleens were extracted and imaged by IVIS.

IVIS imaging

IVIS imaging was used to evaluate the biodistribution experiment. The extracted organs, except for the brains, were imaged ex vivo at an excitation of 640 nm and emission of 680 nm, binning of 4, and f-stop of 2, and 1-s for Cy5-labeled liposome detection (**Figure S18**). Ex vivo images of the brains were obtained at an excitation of 640 nm and emission of 680 nm, binning of 4, and f-stop of 2, and 5-s parameters. The Cy5-labeled BTL (empty) and Cy5-labeled untargeted liposomes were also imaged at 640 nm excitation and 680 nm emission, 4 binning, 2 f-stops, lasting 5 and 1 sec, respectively. Quantitative data from all images were analyzed using the ROI tool in Living Image software. A control (non-injected) mouse was used for analysis; its average radiance was subtracted from the average radiance of each injected tissue, respectively. To compare the BTL (empty) mice group and the untargeted liposomes mice group, the radiance values of each tissue were normalized to the respective mean radiance value of each liposomal formulation.

Analysis of SynO4 antibody levels in the whole brain using an IgG1-based ELISA assay

Mice ~ 4-5 weeks post PD induction (via the injection of 1.5 µl rAAV ($1.63x10^{13}$ GC/ml) directly to the right-side substantia nigra) were randomly separated into three treatment groups: Cy5-labeled BTL loaded with Cy3-labeled SynO4 ($5.59x10^{12}$ particles/ml), free Cy3-labeled SynO4 (158.5 ug/ml), and non-injected. The mice were intravenously injected (150 ul) with the selected treatment and sacrificed 24 hours post-injection. The mice were then perfused with PBS and their brains were frozen using liquid nitrogen and kept at -80°C for further use. Fresh frozen brain tissues were crushed into a fine powder using a pestle and mortar submerged in liquid nitrogen. The frozen powder was then transferred to Ripa Lysis buffer (RIPA; 50 mM Tris-HCL, 150 mM NaCl, 1 mM NP-40, and 0.5mM sodium deoxycholate) supplemented with phosphatase and protease inhibitors – (0.4 mg/ml Collagenase Type 4 (Worthington, USA, LS004186), 0.08 mg/ml Collagenase Type 1 (Sigma-Aldrich, Israel, SCR103) and 0.1 mg/ml DNase 1 (Sigma-Aldrich, Israel, AMPD11KT). After further homogenization, the lysate was centrifuged for 30 min, at 12,000xg, at 4°C. A supernatant containing the entire brain protein lysate was used for the experiment. The protein concentration was measured using the Bradford assay. A protein lysate was produced from each group (i.e., BTL, free SynO4, and no treatment), and 500 ug/ml of total protein from each group was used for the ELISA assay. As the SynO4 antibody is a mouse-origin IgG1 isotype, the detection was performed using an anti-mouse IgG1 Elisa assay kit (Abcam, UK, ab133045), according to the manufacturer's protocol.

Fluorescence immunohistochemistry analysis

Fluorescence histology imaging was used to visually verify the presence of BTL in the brain's substantia nigra area. Mice ~ 4-5 weeks post PD induction (via the injection of 1.5 µl rAAV ($1.63x10^{13}$ GC/ml) directly to the right-side substantia nigra) randomly received one of three treatments: intravenous injection of Cy5-labeled BTL loaded with Cy3-labeled SynO4 ($5.59x10^{12}$ particles/ml), intravenous injection of free Cy3-labeled SynO4 (158.5 ug/ml), and non-injected. The mice were sacrificed 24 hours after the treatment. Finally, they were perfused with PBS, and the brains were frozen using liquid nitrogen and kept at -80°C for further use. Then, 16 µm sections of fresh frozen brain tissue (substantia nigra area) were cut using a cryostat machine. The frozen slices were mounted with DAPI Fluoromount-G (ENCO, Israel, 010020), covered-slipped, and dried overnight at 4ºC. The slides were imaged the following day using confocal microscopy.

Imaging processing, manipulation, and analysis were conducted using Python. To improve the quality of the images and quantify color overlap, several steps were taken. First, a median filter with a kernel size of 5 was applied to reduce noise and create smoother images. Following this, unsharp masking was used to enhance contrast and sharpen edges. The unsharp masked image was generated by subtracting the blurred image from the median filtered image with a weight of 4. Second, channel extraction was performed on the unsharp masked image to separate the red and green color channels. These channels contained pertinent information for quantifying the overlap between respective colors. To determine this overlap, a bitwise AND operation was executed on the red and green channels, resulting in isolated regions where colors overlapped. By converting these overlap regions into binary images and utilizing the OpenCV library, individual contours were identified. The number of contours corresponded directly to the number of overlapping colors within each image analyzed. Finally, all measurements collected from each image were compiled into a data frame and exported as an Excel sheet for further analysis purposes (**Figure S19**).

Transferrin-SynO4 antibody conjugation

Holo-Transferrin Human was cross-linked to SynO4 mAbs by EDC and Sulfo-NHS reagents. First, 1 mg/ml SynO4 antibody solution (PBS), 15 mg/ml Sulfo-NHS (PBS), and 15 mg/ml EDC solution (DMSO) were prepared. Second, the reagent solutions were added to the antibody solution at the following molar proportions: 1:25 SynO4: Sulfo-NHS and 1:10 SynO4: EDC. The pH of the SynO4 solution with the reagents was adjusted to 6, with 1.2M HCL. Then, the solution was mixed (450 rpm) at 25°C for 1 hour. The SynO4 solution was dialyzed against PBS pH 6 (1:1000 volume ratio) using a 12-14 kDa dialysis membrane, at 4ºC, overnight, to remove the excess of the regents. Next, transferrin-SynO4 antibodies were synthesized by mixing 1 mg/ml transferrin solution (PBS) with an activated SynO4 antibody solution at a 2:1 molar proportion, respectively. Then, the pH of the transferrin-SynO4 solution was adjusted to 8.4

with 1M sodium bicarbonate, and the reaction was incubated (450 rpm) for 2 hours, at 25ºC. The non-conjugated transferrin was removed by dialysis against PBS pH 7.4 (1:1000 volume ratio) using a 300 kDa dialysis membrane (Repligen, USA,131456), at 4ºC, for 1 week; the buffer was exchanged twice a day. Finally, a Micro BCA Protein Assay Kit was used to quantify the final concentration of the transferrin-SynO4 antibody solution.

To prepare Cy5-labeled transferrin-SynO4 mAbs, a volume of Cy5-NHS dye was added to a known concentration of transferrin-SynO4 solution, 10:1 molar proportion, respectively. Then, the pH of the Cy5-labeled transferrin-SynO4 solution was adjusted to 8.4 with 1M sodium bicarbonate, and the reaction was incubated (450 rpm), for 2 hours, at 25ºC. Finally, the Cy5-labeled transferrin-SynO4 solution was dialyzed against PBS pH 7.4 (1:1000 volume ratio) using a 12-14 kDa dialysis membrane, at 4ºC, overnight, to remove the excess Cy5 dye.

In-vivo FACS analysis of liposome uptake at the whole brain and the single-cell level

Mice 8 weeks post PD induction (via the injection of 1.5 µl rAAV ($8.15x10^{12}$ GC/ml) directly to the right-side substantia nigra) were intravenously injected either with 350 ul of Cy5-labeled SynO4 (45 ug/ml), with Cy5-labeled transferrin-SynO4 (45 ug/ml) or with Cy5-labeled BTL (empty) ($5.84x10^{12}$ particles/ml); healthy mice were intravenously injected with Cy5-labeled BTL (empty); and non-treated mice were used as a negative control. Twelve hours after injection, the mice were sacrificed and perfused with ice-cold PBS, and their brains were extracted and suspended in cold PBS. The brain tissues were cut into small pieces and enzymatically and physically dissociated using a gentleMACS device (Miltenyi Biotec; it has built-in heating programs provided by S.Shen-Orr lab, Technion) and an Adult Mouse Brain Dissociation Kit, mouse and rat (Almog diagnostics, Israel, 130107677), according to the kit's dissociation protocol.

The dead cells were removed from the cell samples using a Dead Cell Removal Kit (Almog Diagnostics, Israel, 130090101), according to the manufacturer's instructions. The live-single-cell suspensions from each treated brain were divided into "stained" and "non-stained" cells; both groups contained Cy5 dye. The live-single-cell suspensions were divided into "non-stained" and "stained" cells. The "stained" cells were obtained after incubation with a panel of the antibodies PE Anti-Mouse/Human CD44 (Almog diagnostics, Israel, BLG-103008), Brilliant Violet 711™ Anti-Mouse CD45 (Almog diagnostics, Israel, BLG-103147), Brilliant Violet 421™ Anti-Mouse CD31 (Almog diagnostics, Israel, BLG-102424), PE/Cyanine7 Anti-Mouse/Human CD11b (Almog diagnostics, Israel, BLG-101216), Anti-Mouse CD24 Antibody Clone M1/69 Alexa Fluor® 488 (Almog diagnostics, Israel, 60099AD), and ACSA-2 Antibody Anti-Mouse APC-Vio770 REAfinity (Almog diagnostics, Israel, 130-116-247). The dilution of each antibody was determined according to the manufacturer's instructions. The cells were incubated with antibodies for 30 min, on ice, in the dark. Then, they were washed with PB

buffer (0.5% BSA in PBS) once and resuspended with PB buffer before reading. All the cell groups were analyzed using Cytek Aurora; an Anti-Rat and Anti-Hamster Ig k/negative Control Compensation Particles Set (BD, USA, 552845) was used for single staining. A minimum of one million cells were recorded for each test sample. The analysis was performed with FCS Express software (**Figure S20**). The "non-stained" cells of treated brains were used to calculate the average percentage of Cy5-positive cells (**Figure 4F**). The "stained" cells of treated brains were used to calculate the average percentage of Cy5-positive cells within each cell type (**Figure 4G**). The "non-stained" cells of non-treated brains were used to calculate the average percentage of each cell type (cell brain population) (**Figure S21**).

In-vivo FACS analysis of liposome uptake in PD dopaminergic neurons

Mice 8 weeks post PD induction (via the injection of 1.5 µl rAAV ($8.15x10^{12}$ GC/ml) directly to the right-side substantia nigra) were intravenously injected with 350 ul of Cy5-labeled BTL ($9.83x10^{12}$ particles/ml) loaded with Cy3-labeled SynO4 mAbs (80 ug/ml); non-treated mice were used as a negative control. Twelve hours after injection, the mice were sacrificed and perfused with ice-cold PBS, and their brains were extracted and suspended in cold PBS. The brain tissues were cut into small pieces and enzymatically and physically dissociated using a gentleMACS device and an Adult Mouse Brain Dissociation Kit. The dead cells were removed from the cell samples using a Dead Cell Removal Kit. The live-single-cell suspensions from each treated brain were incubated with a panel of the antibodies Brilliant Violet 510™ Anti-Mouse/Human CD44 (Almog diagnostics, Israel, BLG-103044), Brilliant Violet 711™ Anti-Mouse CD45, Brilliant Violet 421™ Anti-Mouse CD31, PE/Cyanine7 Anti-Mouse/Human CD11b, Anti-Dopamine Transporter (DAT) (extracellular)-FITC Antibody (allomone labs, Israel, AMT-003-F), and ACSA-2 Antibody Anti-Mouse APC-Vio770 REAfinity; the incubation of a negative control sample of treated brain was conducted without the Anti-Dopamine Transporter (DAT) (extracellular)-FITC Antibody. The dilution of each antibody was determined according to the manufacturer's instructions. The cells were incubated with antibodies for 35 min, on ice, in the dark. Then, they were washed with PB buffer (0.5% BSA in PBS) once and resuspended with PB buffer before reading. All the cell groups were analyzed using Cytek Aurora; Comp Beads (BioLegend, USA, 424601) was used for single staining. A minimum of one million cells were recorded for each test sample.

Dopaminergic neurons are a rare group, comprising only a small number of approximately 21,000 cells in A summary of the midbrain of C57BL/6 mice[46]. To enhance the likelihood of identifying this population, the FCS files from all six samples were merged using the Cytek Aurora program before conducting the analysis (**Figure S22**).

In-vitro cellular uptake of BTL in PD human dopaminergic neurons

Human dopaminergic neuron cells were treated with 2.5mM Cy5-labeled BTL particles in 500 ul media per well. This 48-hour treatment was carried out 45 days after patient derivation. Subsequently, the neurons were fixed with 4% paraformaldehyde at 37°C for 15 minutes, followed by three washes with PBS for 5 minutes each.

For immunocytochemistry[47], the fixed neurons on 48-well coverslips were subjected to a 1-hour treatment with 0.2% Triton-X for permeabilization and then blocked using 10% horse serum in DPBS. The primary antibodies, mouse Tyrosine Hydroxylase antibody (Abcam, UK, ab129991) at a 1/250 dilution, and chicken beta-III-tubulin/TUJ1 (Abcam, UK, ab41489) at a 1/1500 dilution, were applied to the cells and incubated. For secondary antibody staining, a Goat Anti-Mouse IgG (H&L)-488 (Abcam, UK, ab150117) and a Goat Anti-Chicken IgY (H&L)-568 (Abcam, UK, ab175711) were used at dilutions of 1/250 and 1/1000, respectively.

The coverslips were counterstained with DAPI using Fluoromount-GTM Mounting Medium (Thermo Fisher Scientific, USA, 00-4959-52) and left to dry overnight, protected from light. The imaging process was conducted at the LSE infrastructure center (Technion) using ZEN software with lasers at 405nm, 488nm, 543nm, and 639nm wavelengths. Confocal z-stacks were acquired for analysis. Additionally, antibody controls were treated under the same conditions except that they were not incubated with primary antibodies (**Figure 4H**).

In-vivo therapeutic efficacy

Mice received a unilateral stereotactic injection of 1.5 µL AAV vector encoding human alpha-synuclein at a concentration of $8.15x10^{12}$ GC/ml. The mice were randomly divided into the following four groups (4-5 mice per group): healthy (non-injected with viral vector), untreated (PD), PD with BTL recipients, and PD with free SynO4 mAb recipients. Cy5-labeled BTL (250 ul of 50 mM liposomes (0.5 mg/kg body weight of encapsulated antibody)) or SynO4 antibody (250 ul of 40 ug/ml solution (0.5 mg/kg)) were injected intravenously every other day for a period of 2 and 4 weeks; the mice's weight was monitored. Finally, the mice were sacrificed and perfused, and their brains were harvested, fixed (PFA 4%, neutral-buffered, for at least 24 hours), and further examined.

Immunohistochemistry analysis

Fixed brain specimens were embedded in paraffin and the substantia nigra and striatum (CP) areas were sectioned into 5-um-thick slices. Next, tissue sections were deparaffinized in a xylene ethanol gradient (xylene, xylene/ethanol (1:1 v/v), absolute ethanol, 95% ethanol, 70% ethanol, and 50% ethanol) for 3 min each and then placed in distilled water (DW). Antigen retrieval was done in 10 mM tri-sodium citrate solution at pH 6 tittered with HCl. Ready-to-

use normal goat serum (2.5%) was used for blocking. Next, the sections were incubated at 4ºC, overnight, with one of the following primary mAbs; Chicken Anti-Tyrosine Hydroxylase (1:1000; Abcam, UK, ab76442), Mouse-Anti Aggregated Alpha-Synuclein Clone 5G4 (1:400; Mercury Scientific, Israel, MABN389), or Rabbit Anti-Iba1 (1:2000; Abcam, UK, ab178846), Rabbit Anti-GFAP (1:2000; Abcam, UK, ab68428). Next, the tissue sections were rinsed with DW and then incubated for 30 min, in 0.3% H2O2 solution, to block endogenous peroxidase activity. The tissue sections were then washed in DW and incubated for 40 min, at room temperature, with either Goat Anti-Chicken IgY (HRP) (Abcam, UK, ab6877), ImmPRESS Goat Anti-Rabbit IgG (HRP) (Vector Laboratories, USA, VE-MP-7451-50), or Goat Anti-Mouse IgG (HRP) antibody. Next, the tissue sections were rinsed 3 times with DW and then, for color development, were incubated with DAB solution (Vector Laboratories, USA, SK4105 kit) for 2 min, washed with DW, and counterstained with hematoxylin. By staining alpha-synuclein aggregates first and then incubating chicken anti-tyrosine hydroxylase for 1 hour at room temperature, we were able to double-stain dopaminergic neurons (anti-tyrosine hydroxylase) and AS aggregates (5G4 clone) simultaneously (**Figure S23**). Shortly after the AS staining, the tissue sections were rinsed with DW and then incubated with the anti-chicken HRP antibody, for 40 min, at RT. Next, they were rinsed three times with DW and incubated with vector red solution (Vector Laboratories, USA, SK-5105 kit), for 25 min, for color development. Finally, the tissue sections were washed with DW and counterstained with hematoxylin.

All the slides were scanned using a 3DHistech Panoramic 250 Flash III automated slide scanner. The area with the viable regions (annotations) was measured using CaseViewer software and used for further analysis.

Imaging analysis of immunohistochemistry staining

The image processing was performed by the image analysis team at the Biomedical Core Facility, Technion. The analysis was conducted using Python, utilizing several images and data processing libraries, and based on several consecutive steps for each image. The first step of the analysis included color segmentation. Herein, the brown-colored areas were counted and compared to the overall area of the tissue. The next step consisted of structure segmentation based on a pre-trained convolutional neural network (CNN), where cells were detected and counted. Third, the colocalization of brown color expression and cell structure in the image was quantified for counting the brown color-expressed cells. Finally, the measurements for each image were collected as a data frame and exported as an Excel sheet for further analysis (**Figure 5B, C, and D, and Figures S23, 24, 25, and 26**). In the same brain section, the percentage of neuronal loss was calculated by dividing the number of dopaminergic neurons found in the right hemisphere (viral-injected side) by the number of dopaminergic neurons located in the left hemisphere (non-viral injected side). Next, the values of the healthy group

were normalized to 1, and the values of all the other groups were normalized to the healthy group's mean value.

Evaluation of behavioral changes in PD mice post viral inducing

Healthy 6-8-week-old male c57BC/6JRccHsd mice were kept on a regular 12-hour light/dark cycle (light phase: 7 AM to 7 PM) in a controlled environment (22ºC, 50% humidity) with water and food ad libitum. First, to establish an accurate model for a behavioral test, the mice were divided into 3 groups: healthy controls, mice injected with $8.15x10^{12}$ GC/ml of AAV viruses (concentration used in the previous biochemical experiments), and mice injected with $1.08x10^{13}$ GC/ml of AAV viruses. To evaluate coordination and balance functions, we measured the motor activity of the mice at 7, 21, and 35 days post-viral injection, using an accelerating speed rotarod (**Figure S28**). The low concentration of AAV viruses was not found to cause a significant reduction in the latency to fall, indicating a motor performance comparable to that of the healthy controls (Day 7 p=4942; Day 21 p=0.8232; Day 35 p=0.9952). On the other hand, 35 days after the high viral concentration injection, a significant reduction in latency to fall was observed (p<0.0165). As a result, the high viral concentration was used in the behavioral experiments to test the therapeutic efficacy of BTL.

In the behavioral experiments, the mice were randomly divided into four groups (7-8 mice each) as follows: healthy (non-injected with viral vector), PD untreated, BTL, and free SynO4. Cy5-labeled BTL (350 ul of 50 mM liposomes; 0.5 mg/kg body weight of encapsulated antibody) or free SynO4 mAbs (250 ul of 40 ug/ml solution; 0.5 mg/kg) were injected intravenously every other day for 4 weeks. The weight of the mice was monitored.

The rotor-rod apparatus (San Diego Instruments, San Diego, CA) is made of a black Perspex material featuring a horizontal rotating rod (5.5 cm diameter) that consists of four lanes with opaque black Perspex dividers for each mouse. The apparatus also includes a sawdust cabin (45.7 cm height) for safe landing. The red-beam system automatically records fall latencies in seconds to accurately assess the animal's performance.

To assess the efficacy of the BTL vs. free SynO4, we utilized the Rotor-rod test. This test is commonly used to evaluate motor function and learning in rodents.[48] One week post viral injection, the mice were handled daily (~6 min) and habituated to the experimenter and experimental room, for a week. The Rotor-rod test was conducted during the third and fifth post-injection weeks (after 2 and 4 weeks of treatment) by a trained experimenter blinded to the treatment conditions. During each experimental week, the test was performed on three consecutive days, with four daily trials separated by a 2-minute inter-trial interval. The experimental and control naive groups were evaluated between 9:00 AM-12:00 PM in a counterbalanced manner to avoid a testing order/time effect between the groups. On the

first day of the experiment, each mouse was placed on the rod for 2 min, allowing habituation to the arena before the test began. During each trial, the initial rotation speed of the rod was 5 rpm for 15 sec, which gradually accelerated at a rate of 0.1 rpm/sec up to a maximum speed of 50 rpm after 450 sec. The latency to fall was recorded for each trial, and a mean was calculated for each mouse per testing day, to provide a quantitative measure of the motor performance. The average latency of the first testing day served as an indication of motor functioning while the last testing day was used as a representation of the motor learning endpoint. All the motor measurements were performed in a double-blind manner and the identification of the groups was only revealed at the end of the experiment.

Analyzing toxicity using immunohistochemistry

Fixed organs' (liver, kidneys, and spleen) specimens were embedded in paraffin and sectioned into 5-um-thick sections. Next, the tissue sections were deparaffinized in a xylene ethanol gradient (xylene, xylene/ethanol (1:1 v/v), absolute ethanol, 95% ethanol, 70% ethanol, and 50% ethanol) for 3 minutes each and then placed in distilled water (DW). Sections were stained with hematoxylin for nuclear stain, rinsed in tap water, and then stained with 1% eosin.

All the slides were scanned using a 3DHistech Panoramic 250 Flash III automated slide scanner. The area of the viable regions (annotations) was measured using CaseViewer software and used for further analysis.

Hematology blood test

After 4 weeks of the behavior experiment, i.e., 40 days after the experiment began, blood samples were collected from mice. The mice were sacrificed and terminally bled through a cardiac puncture. To analyze the chemistry parameters, blood samples were incubated on ice for 30 minutes, followed by centrifugation for 10 minutes at 10,000 rpm to separate the serum. A heparin-coated syringe was used to collect blood samples into EDTA-covered vials to prevent the formation of clots. An analysis of blood cell count and multiple chemistry parameters was conducted (American Medical Laboratories, Israel) to evaluate systemic immunogenicity, inflammation, hepatotoxicity, and nephrotoxicity of BTL and free SynO4 treatment. All values were normalized to the healthy control group.

Statistical analysis

All data were reported as the mean ± standard deviation (mean±SD). Comparisons were made between distinct groups. Groups were analyzed by a two-tailed unpaired t-test, one-way analysis of variance (ANOVA), and two-way analysis of variance (ANOVA). Statistical significance was set as *p<0.05, **p <0.01, ***p<0.001, and ****p<0.0001, with a 95% confidence interval. Analysis and figures were generated using GraphPad Prism v. 8.0 software.

Acknowledgments

We thank Mrs. Irina Davidovich and Dr. Naama Koifman from the Technion Center for Electron Microscopy of Soft Matter for the cryo-TEM measurements, Dr. Nitsan Dahan, Dr. Yael Lupu-Haber, Dr. Aviv Lutaty and Yousef Mansour from the Life Sciences and Engineering Infrastructure Center Emerson Building for Life Sciences, Technion, and Mr. Ariel Shemesh, Mrs. Sana Huleilhel, Mrs. Katren Sakran and Maya Holdengreber from the Biomedical Core Facility, Technion, to Dr. Tatiana Rabinski for assisting with the iPSC preparation from Tel Aviv University and to Ms. Natalie Page for proofreading of the article. The images in this paper were created with BioRender.com and Adobe Illustrator.

Funding: This research was supported by funds from the European Union Horizon Europe research and innovation program (grant agreement No. 101089009-ERC- [4D Brain-Targeting Nanomedicines for Treating Neurodegeneration]; Israel Innovation Authority Nofar Grant (67967, 75626); Israel Science Foundation (1881/21); Israel Ministry of Science, Technology & Space (3-16963; 3-17418); Leventhal 2020 COVID19 Research Fund (ATS #11947); German-Israeli Foundation for Scientific Research and Development GIF Young grant (I-2328-1139.10/2012); European Union FP-7 IRG Program for a Career Integration (grant No. 908049); Phospholipid Research Center (grant No. ASC-2018-062/1-1); Ministry of Agriculture & Rural Development, Office of the Chief Scientist (323/19); Teva Pharmaceutical Industries Ltd.; Louis family Cancer Research Fund; Mallat Family Foundation Grant; Unger Family Fund; Carrie Rosenblatt Cancer Research Fund; ERC SweetBrain 851765; The Aufzien Family Center for the Prevention and Treatment of Parkinson's Disease at Tel Aviv University (to BMM and UA); the Zimmin Foundation (to BMM and UA); TEVA Pharmaceuticals (to BMM and UA); Israel Ministry of Science and Technology (Grant No. 3–17351) (to BMM); Israel Science Foundation (ISF grant: 2248/19 and 1934/23) (to BMM); BrightFucos grant (A2022029S) (to UA); NIH grant 1R21AG074846-01A1 (to UA); the Michael J. Fox Foundation (MJFF-022407) (to UA); Israel Science Foundation (ISF grant: 2141/20) (to UA); Ministry of Innovation, Science & Technology, Israel (1001576154) (to UA); The Zuckerman STEM leadership program (to UA and SS); the European Union Horizon Europe research (grant agreement No. 101088881, 2022-COG) (to A.B.Z); Israel Science Foundation (2359/23) (to ABZ); ERC-Stg grant (2CE-

MECP2 No. 101040128) (to T.L); ISF grant (1384/21) (to T.L). A. Schroeder acknowledges Alon and Taub fellowships. Furthermore, the authors would like to acknowledge the Technion's Integrated Cancer Center, Russell Berrie Nanotechnology Institute (RBNI), Lorry I. Lokey Interdisciplinary Center for Life Sciences & Engineering, and Biomedical Core Facility. Mor Sela and Maya Kaduri wish to thank TEVA Pharmaceuticals and NFBI (The National Forum for Bio-Innovators) for their Doctoral Fellowships. Maya Kaduri also wishes to thank the Technion Integrated Cancer Center for a Rubinstein scholarship and the Robert B. Kalmansohn Fellowship Fund in the Emerson Life Sciences Building. Maria Poley wishes to thank the Israeli Ministry of Science and Technology for a Shulamit Aloni Doctoral Fellowship. Patricia Mora-Raimundo wishes to thank the Azrieli Foundation for a Post-Doctoral Fellowship. Aviram Avital wishes to thank the Jewish National Fund (KKL-JNF) Climate Scholarships. Omer Adir wishes that thank the Jacob and Gutwirth Fellowships.

Author contributions: A.S. supervised and directed the research. M.S., M.P., and P.M.R. wrote the manuscript and designed, performed, and analyzed all the experiments. S.K. helped perform some of the *in-vitro* and *in-vivo* experiments. A.A. performed the RT-PCR assay. M.K. helped perform and analyze some of the *in-vitro* experiments. G.C. helped perform some of the *in-vivo* experiments. O.A. wrote the code for the cryo-TEM imaging analysis. A.R. assisted with some of the *in-vitro* and *in-vivo* experiments. B.M.M. and Y.L.B. helped design and conduct the BBB liposome cross experiments. U.A. and Y.W. helped design and conduct experiments with the primary neurons. O.S. was involved in the dSTORM image analysis. A.A., L.S., and S.A.M. helped design and conduct the behavior experiments. A.B.Z, B.B., and Y.Y.P. planned and performed experiments on the intracellular distribution of BTL in mice brain endothelial cells and evaluated the BTL lysosomal escape. T.L. and A.Z.O. performed the spatial and temporal dynamics of BTL entry into neurons in the brain. S.S., A.C., I.R., and D.C. helped design and conduct the BTL cellular uptake experiments in human dopaminergic neuron cells. A.A., S.C.A., and Y.B. designed the plasmid used in the *in vitro* imaging of BTL uptake. D.H. and J.E.S. assisted with the analysis results of the safety experiments. P.H. and A.O. assisted with image analysis and quantification of the BTL signal in brain histology sections. J.S. and J.S.R. assisted in data analysis and funding obtaining. All authors helped to improve the manuscript.

Competing interests: The authors declare that they have no competing interests.

Data and materials availability: All the data needed to evaluate the conclusions in the paper are present in the paper and/or the Supplementary Materials. Correspondence and requests for materials should be addressed to A.S. (avids@technion.ac.il)

References

[1] a)L. S. Forno, in *Progress in Parkinson Research*, Springer, 1988; b)D. J. Surmeier, *The Lancet Neurology* **2007**, 6, 933.

[2] W. Poewe, K. Seppi, C. M. Tanner, G. M. Halliday, P. Brundin, J. Volkmann, A.-E. Schrag, A. E. Lang, *Nature reviews Disease primers* **2017**, 3, 1.

[3] T.-I. Kam, J. T. Hinkle, T. M. Dawson, V. L. Dawson, *Neurobiology of disease* **2020**, 144, 105028.

[4] L. M. De Lau, M. M. Breteler, *The Lancet Neurology* **2006**, 5, 525.

[5] M. G. Spillantini, M. L. Schmidt, V. M.-Y. Lee, J. Q. Trojanowski, R. Jakes, M. Goedert, *Nature* **1997**, 388, 839.

[6] J. Burré, M. Sharma, T. C. Südhof, *Journal of Neuroscience* **2015**, 35, 5221.

[7] F. Miraglia, A. Ricci, L. Rota, E. Colla, *Neural Regeneration Research* **2018**, 13, 1136.

[8] C. R. Fields, N. Bengoa-Vergniory, R. Wade-Martins, *Frontiers in molecular neuroscience* **2019**, 12, 299.

[9] a)E. Masliah, E. Rockenstein, M. Mante, L. Crews, B. Spencer, A. Adame, C. Patrick, M. Trejo, K. Ubhi, T. T. Rohn, *PloS one* **2011**, 6, e19338; b)D. Games, E. Valera, B. Spencer, E. Rockenstein, M. Mante, A. Adame, C. Patrick, K. Ubhi, S. Nuber, P. Sacayon, *Journal of Neuroscience* **2014**, 34, 9441; c)E. Valera, E. Masliah, *Pharmacology & therapeutics* **2013**, 138, 311.

[10] O. El-Agnaf, C. Overk, E. Rockenstein, M. Mante, J. Florio, A. Adame, N. Vaikath, N. Majbour, S.-J. Lee, C. Kim, *Neurobiology of disease* **2017**, 104, 85.

[11] a)J. O. Szablowski, A. Bar-Zion, M. G. Shapiro, *Accounts of chemical research* **2019**, 52, 2427; b)X. Cai, M. Chen, A. Prominski, Y. Lin, N. Ankenbruck, J. Rosenberg, M. Nguyen, J. Shi, A. Tomatsidou, G. Randall, *Advanced Science* **2022**, 9, 2103240.

[12] a)H. Kadry, B. Noorani, L. Cucullo, *Fluids and Barriers of the CNS* **2020**, 17, 1; b)B. T. Hawkins, T. P. Davis, *Pharmacological reviews* **2005**, 57, 173.

[13] D. Tarab-Ravski, I. Hazan-Halevy, M. Goldsmith, L. Stotsky-Oterin, D. Breier, G. S. Naidu, A. Aitha, Y. Diesendruck, B. D. Ng, H. Barsheshet, *Advanced Science* **2023**, 2301377.

[14] a)S. A. Dilliard, Q. Cheng, D. J. Siegwart, *Proceedings of the National Academy of Sciences* **2021**, 118, e2109256118; b)C. Ferro, H. F. Florindo, H. A. Santos, *Advanced healthcare materials* **2021**, 10, 2100598; c)G. Sahay, D. Y. Alakhova, A. V. Kabanov, *Journal of controlled release* **2010**, 145, 182.

[15] a)B. Gupta, V. P. Torchilin, *Cancer immunology, immunotherapy* **2007**, 56, 1215; b)B. Gupta, T. S. Levchenko, V. P. Torchilin, *Oncology Research Featuring Preclinical and Clinical Cancer Therapeutics* **2006**, 16, 351; c)O. Veiseh, C. Sun, C. Fang, N. Bhattarai, J. Gunn, F. Kievit, K. Du, B. Pullar, D. Lee, R. G. Ellenbogen, *Cancer research* **2009**, 69, 6200; d)J. Xu, X. Wang, H. Yin, X. Cao, Q. Hu, W. Lv, Q. Xu, Z. Gu, H. Xin, *ACS nano* **2019**, 13, 8577; e)D. E. Tylawsky, H. Kiguchi, J. Vaynshteyn, J. Gerwin, J. Shah, T. Islam, J. A. Boyer, D. R. Boué, M. Snuderl, M. B.

Greenblatt, *Nature Materials* **2023**, 22, 391; f)O. Betzer, N. Perets, A. Angel, M. Motiei, T. Sadan, G. Yadid, D. Offen, R. Popovtzer, *ACS nano* **2017**, 11, 10883; g)O. Betzer, M. Shilo, M. Motiei, R. Popovtzer, presented at *Nanoscale Imaging, Sensing, and Actuation for Biomedical Applications XVI*, **2019**; h)T. Lammers, P. Koczera, S. Fokong, F. Gremse, J. Ehling, M. Vogt, A. Pich, G. Storm, M. Van Zandvoort, F. Kiessling, *Advanced functional materials* **2015**, 25, 36; i)J.-N. May, S. K. Golombek, M. Baues, A. Dasgupta, N. Drude, A. Rix, D. Rommel, S. Von Stillfried, L. Appold, R. Pola, *Theranostics* **2020**, 10, 1948; j)T. Lammers, P. Koczera, S. Fokong, F. Gremse, J. Ehling, M. Vogt, A. Pich, G. Storm, M. van Zandvoort, F. Kiessling, *Advanced Functional Materials* **2015**, 25, 2; k)Z. Li, Y. Zhu, H. Zeng, C. Wang, C. Xu, Q. Wang, H. Wang, S. Li, J. Chen, C. Xiao, *Nature Communications* **2023**, 14, 1437.

[16] a)S. A. Attia, X. Li, N. Filipczak, D. F. Costa, V. P. Torchilin, in *Peptide Conjugation*, Springer, 2021; b)K. B. Johnsen, M. Bak, P. J. Kempen, F. Melander, A. Burkhart, M. S. Thomsen, M. S. Nielsen, T. Moos, T. L. Andresen, *Theranostics* **2018**, 8, 3416; c)K. B. Johnsen, M. Bak, F. Melander, M. S. Thomsen, A. Burkhart, P. J. Kempen, T. L. Andresen, T. Moos, *Journal of Controlled Release* **2019**, 295, 237.

[17] a)V. M. Pulgar, *Frontiers in neuroscience* **2019**, 12, 1019; b)Y. J. Yu, Y. Zhang, M. Kenrick, K. Hoyte, W. Luk, Y. Lu, J. Atwal, J. M. Elliott, S. Prabhu, R. J. Watts, *Science translational medicine* **2011**, 3, 84ra44.

[18] G. Gregoriadis, Y. Perrie, *eLS* **2010**.

[19] M. J. Fischer, in *Surface plasmon resonance*, Springer, 2010.

[20] a)J. Jumper, R. Evans, A. Pritzel, T. Green, M. Figurnov, O. Ronneberger, K. Tunyasuvunakool, R. Bates, A. Žídek, A. Potapenko, *Nature* **2021**, 596, 583; b)M. Varadi, S. Anyango, M. Deshpande, S. Nair, C. Natassia, G. Yordanova, D. Yuan, O. Stroe, G. Wood, A. Laydon, *Nucleic acids research* **2022**, 50, D439; c)B. E. Eckenroth, A. N. Steere, N. D. Chasteen, S. J. Everse, A. B. Mason, *Proceedings of the National Academy of Sciences* **2011**, 108, 13089.

[21] J. F. Stefanick, J. D. Ashley, T. Kiziltepe, B. Bilgicer, *ACS nano* **2013**, 7, 2935.

[22] J. S. Suk, Q. Xu, N. Kim, J. Hanes, L. M. Ensign, *Advanced drug delivery reviews* **2016**, 99, 28.

[23] a)M. Kaduri, M. Sela, S. Kagan, M. Poley, H. Abumanhal-Masarweh, P. Mora-Raimundo, A. Ouro, N. Dahan, D. Hershkovitz, J. Shklover, *Science advances* **2021**, 7, eabj5435; b)A. Zinger, C. Cvetkovic, M. Sushnitha, T. Naoi, G. Baudo, M. Anderson, A. Shetty, N. Basu, J. Covello, E. Tasciotti, *Advanced Science* **2021**, 8, 2101437; c)T. T. Goodman, C. P. Ng, S. H. Pun, *Bioconjugate chemistry* **2008**, 19, 1951.

[24] B. Bell, S. Anzi, E. Sasson, A. Ben-Zvi, *Fluids and Barriers of the CNS* **2023**, 20, 1.

[25] T. Saito, N. Nakatsuji, *Developmental biology* **2001**, 240, 237.

[26] T. Laviv, B. Scholl, P. Parra-Bueno, B. Foote, C. Zhang, L. Yan, Y. Hayano, J. Chu, R. Yasuda, *Neuron* **2020**, 105, 799.

[27] S.-D. Li, L. Huang, *Molecular pharmaceutics* **2008**, 5, 496.

[28] a)C. Morris, J. Candy, S. Omar, C. Bloxham, J. Edwardson, *Neuropathology and applied neurobiology* **1994**, 20, 468; b)A. D'Souza, S. Nozohouri, B. S. Bleier, M. M. Amiji, *Pharmaceutical Research* **2023**, 40, 77.

[29] B. A. Faucheux, J.-J. Hauw, Y. Agid, E. C. Hirsch, *Brain research* **1997**, 749, 170.

[30] B. A. Hijaz, L. A. Volpicelli-Daley, *Molecular neurodegeneration* **2020**, 15, 1.

[31] L. Ma, M. Gholam Azad, M. Dharmasivam, V. Richardson, R. Quinn, Y. Feng, D. Pountney, K. Tonissen, G. Mellick, I. Yanatori, 2021.

[32] S. Stern, S. Lau, A. Manole, I. Rosh, M. M. Percia, R. Ben Ezer, M. N. Shokhirev, F. Qiu, S. Schafer, A. A. Mansour, *npj Parkinson's Disease* **2022**, 8, 103.

[33] A. K. Lakkaraju, S. Sorce, A. Senatore, M. Nuvolone, J. Guo, P. Schwarz, R. Moos, P. Pelczar, A. Aguzzi, *Brain Pathology* **2022**, e13056.

[34] a)J. Ridet, A. Privat, S. Malhotra, F. Gage, *Trends in neurosciences* **1997**, 20, 570; b)W. Kang, J. M. Hébert, *Molecular neurobiology* **2011**, 43, 147; c)X.-L. Gu, C.-X. Long, L. Sun, C. Xie, X. Lin, H. Cai, *Molecular brain* **2010**, 3, 1; d)M. E. Hamby, M. V. Sofroniew, *Neurotherapeutics* **2010**, 7, 494.

[35] a)A. M. Jurga, M. Paleczna, K. Z. Kuter, *Frontiers in cellular neuroscience* **2020**, 14, 198; b)K. Hopperton, D. Mohammad, M. Trépanier, V. Giuliano, R. Bazinet, *Molecular psychiatry* **2018**, 23, 177.

[36] J. C. Masters, D. J. Nickens, D. Xuan, R. L. Shazer, M. Amantea, *Investigational New Drugs* **2018**, 36, 121.

[37] H. Allen Reish, D. Standaert, DOI 10.3233/JPD-140491, 2015.

[38] a)T. Moos, T. R. Nielsen, T. Skjørringe, E. H. Morgan, *Journal of neurochemistry* **2007**, 103, 1730; b)Y. J. Yu, J. K. Atwal, Y. Zhang, R. K. Tong, K. R. Wildsmith, C. Tan, N. Bien-Ly, M. Hersom, J. A. Maloney, W. J. Meilandt, *Science translational medicine* **2014**, 6, 261ra154.

[39] J. Schindelin, I. Arganda-Carreras, E. Frise, V. Kaynig, M. Longair, T. Pietzsch, S. Preibisch, C. Rueden, S. Saalfeld, B. Schmid, *Nature methods* **2012**, 9, 676.

[40] A. Lavi, A. Sheinin, R. Shapira, D. Zelmanoff, U. Ashery, *Cerebral Cortex* **2014**, 24, 2309.

[41] a)E. H. Neal, N. A. Marinelli, Y. Shi, P. M. McClatchey, K. M. Balotin, D. R. Gullett, K. A. Hagerla, A. B. Bowman, K. C. Ess, J. P. Wikswo, *Stem cell reports* **2019**, 12, 1380; b)G. D. Vatine, R. Barrile, M. J. Workman, S. Sances, B. K. Barriga, M. Rahnama, S. Barthakur, M. Kasendra, C. Lucchesi, J. Kerns, *Cell stem cell* **2019**, 24, 995.

[42] R. Rauti, A. Ess, B. Le Roi, Y. Kreinin, M. Epshtein, N. Korin, B. M. Maoz, *APL bioengineering* **2021**, 5.

[43] a)L. Barna, B. Dudok, V. Miczán, A. Horváth, Z. I. László, I. Katona, *Nature protocols* **2016**, 11, 163; b)G. T. Dempsey, J. C. Vaughan, K. H. Chen, M. Bates, X. Zhuang, *Nature methods* **2011**, 8, 1027; c)J. Zhang, C. M. Carver, F. S. Choveau, M. S. Shapiro, *Neuron* **2016**, 92, 461.

[44] M. Ovesný, P. Křížek, J. Borkovec, Z. Švindrych, G. M. Hagen, *Bioinformatics* **2014**, 30, 2389.

[45] C. A. Schneider, W. S. Rasband, K. W. Eliceiri, *Nature methods* **2012**, 9, 671.
[46] W. Menegas, J. F. Bergan, S. K. Ogawa, Y. Isogai, K. Umadevi Venkataraju, P. Osten, N. Uchida, M. Watabe-Uchida, *Elife* **2015**, 4, e10032.
[47] B. Brant, T. Stern, H. A. Shekhidem, L. Mizrahi, I. Rosh, Y. Stern, P. Ofer, A. Asleh, G. K. E. Umanah, R. Jada, *Molecular psychiatry* **2021**, 26, 7498.
[48] a)E. Kaplan, S. Zubedat, I. Radzishevsky, A. C. Valenta, O. Rechnitz, H. Sason, C. Sajrawi, O. Bodner, K. Konno, K. Esaki, *Proceedings of the National Academy of Sciences* **2018**, 115, 9628; b)S. Zubedat, Y. Freed, Y. Eshed, A. Cymerblit-Sabba, A. Ritter, M. Nachmani, R. Harush, S. Aga-Mizrachi, A. Avital, *Neuroscience* **2013**, 253, 1; c)H. Rosenmann, N. Grigoriadis, H. Eldar-Levy, A. Avital, L. Rozenstein, O. Touloumi, L. Behar, T. Ben-Hur, Y. Avraham, E. Berry, *Experimental neurology* **2008**, 212, 71; d)T. Wang, N. Yasin, S. Zubedat, Y. Loboda, A. Avital, L. Schachter, J. P. Finberg, *Brain Research Bulletin* **2022**, 189, 111.

Table of Contents

Mor Sela, Maria Poley, Patricia Mora-Raimundo, Shaked Kagan, Aviram Avital, Maya Kaduri, Gal Chen, Omer Adir, Adi Rozencweig, Yfat Weiss, Ofir Sade, Yael Leichtmann-Bardoogo, Lilach Simchi, Shlomit Age-Mizrachi, Batia Bell, Yoel Yeretz-Peretz, Aviv Zaid Or, Ashwani Choudhary, Idan Rosh, Diogo Cordeiro, Stav Choen-Adiv, Yevgeny Berdichevsky, Anas Ode Jeny Shklover, Janna Shainsky-Roitman, Joshua E. Schroeder, Dov Hershkovitz, Peleg Hasson, Avraham Ashkenazi, Shani Stern, Tal Laviv, Ayal Ben-Zvi, Avi Avital, Uri Ashery, Ben M. Maoz and Avi Schroeder

Brain-targeted liposomes loaded with monoclonal antibodies reduce alpha-synuclein aggregation and improve behavioral symptoms of Parkinson's disease

The authors highlight a targeted drug delivery system for treating Parkinson's disease. By engineering brain-targeted liposomes with transferrin on the outer surface of the nanoparticles, and containing therapeutic antibodies, they achieve successful crossing of the blood-brain-barrier and effective treatment of brain neurons. This approach reduces alpha-synuclein aggregation and neuroinflammation, showcasing its potential for delivering biologics in the treatment of neurodegenerative diseases.